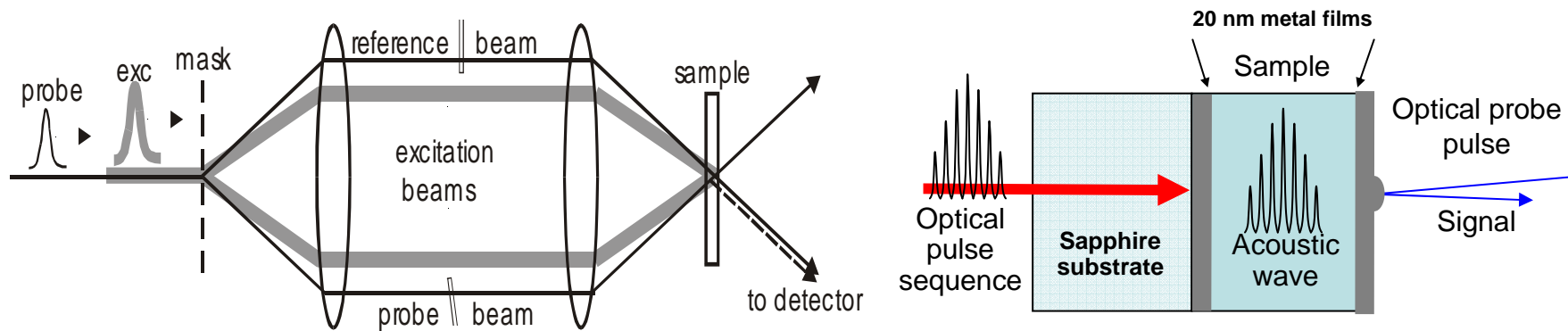


Acoustic wave spectroscopy across the Brillouin zone

Optical excitation of acoustic waves through wavevector and frequency specification



Jeremy Johnson, Darius Torchinsky Christoph Klieber, Thomas Pezeril

Keith A. Nelson Research Group
Department of Chemistry
MIT

Outline

Acoustic wave generation & detection

MHz frequency range

Impulsive stimulated Brillouin, thermal scattering

Longitudinal & shear waves

GHz frequency range

Multiple-pulse picosecond ultrasonics

Longitudinal & shear waves

Supercooled liquids & glasses

Tests of mode-coupling theory

Tests of “shoving” model & Poisson ratio prediction

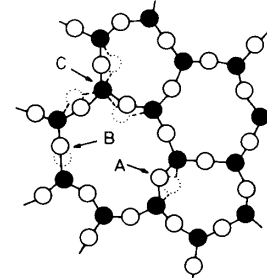
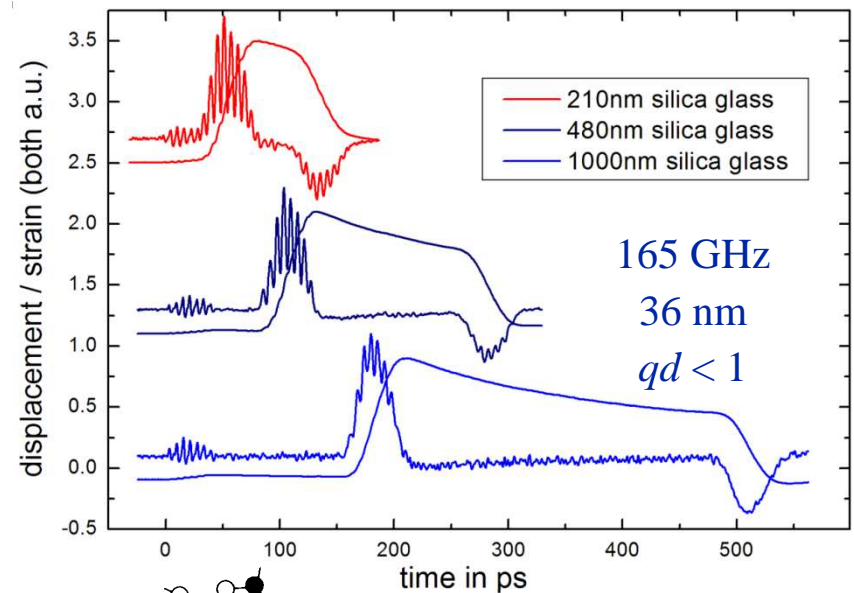
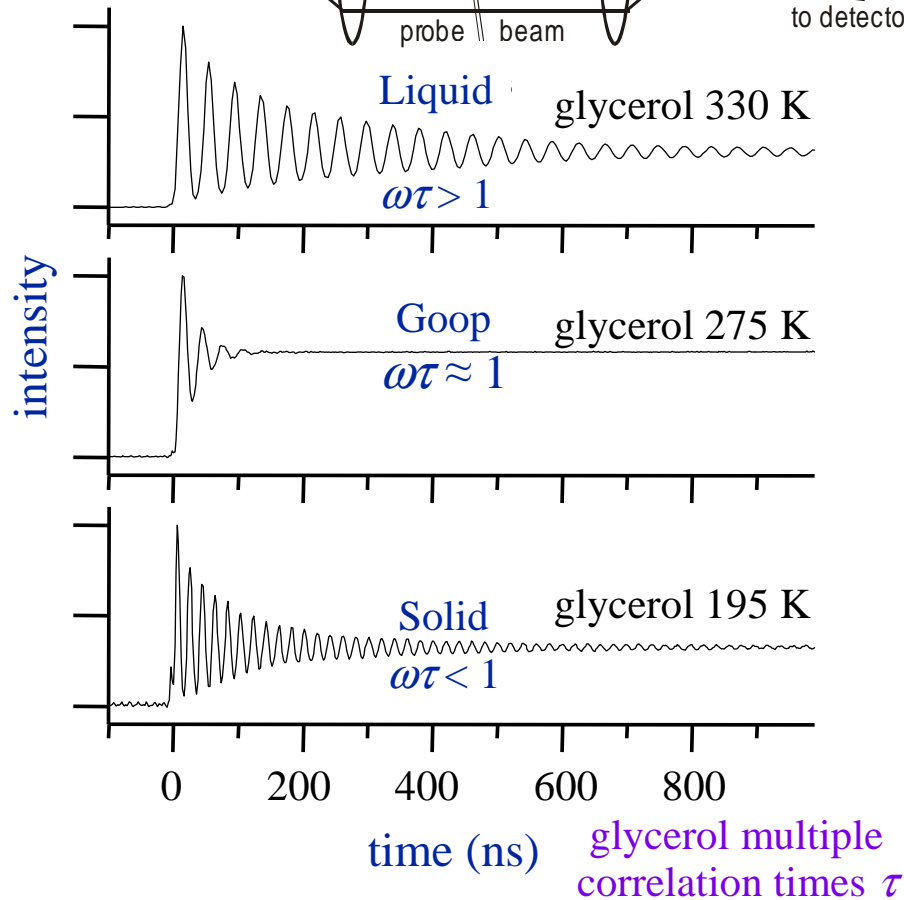
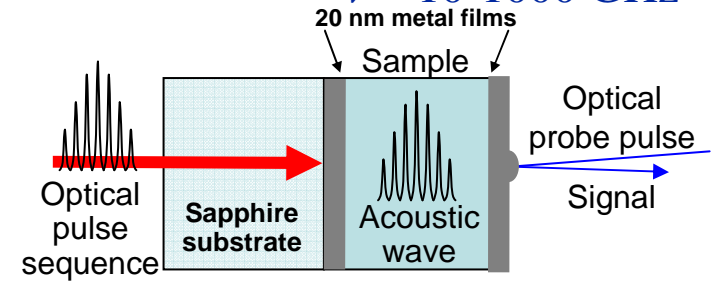
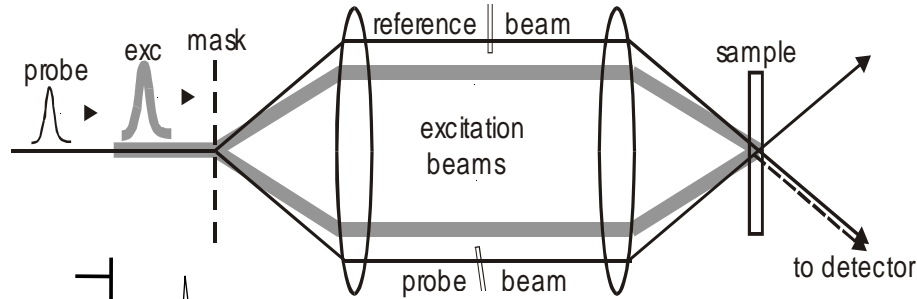
Comparison between longitudinal & shear dynamics

Acoustic waves at all frequencies & wavelengths

Two approaches for MHz and GHz ranges

Crossed beams \Rightarrow $\lambda = 1-200 \mu\text{m}$
 $\nu = 10-1000 \text{ MHz}$

Multiple pulses \Rightarrow $\lambda = 5-500 \text{ nm}$
 $\nu = 10-1000 \text{ GHz}$

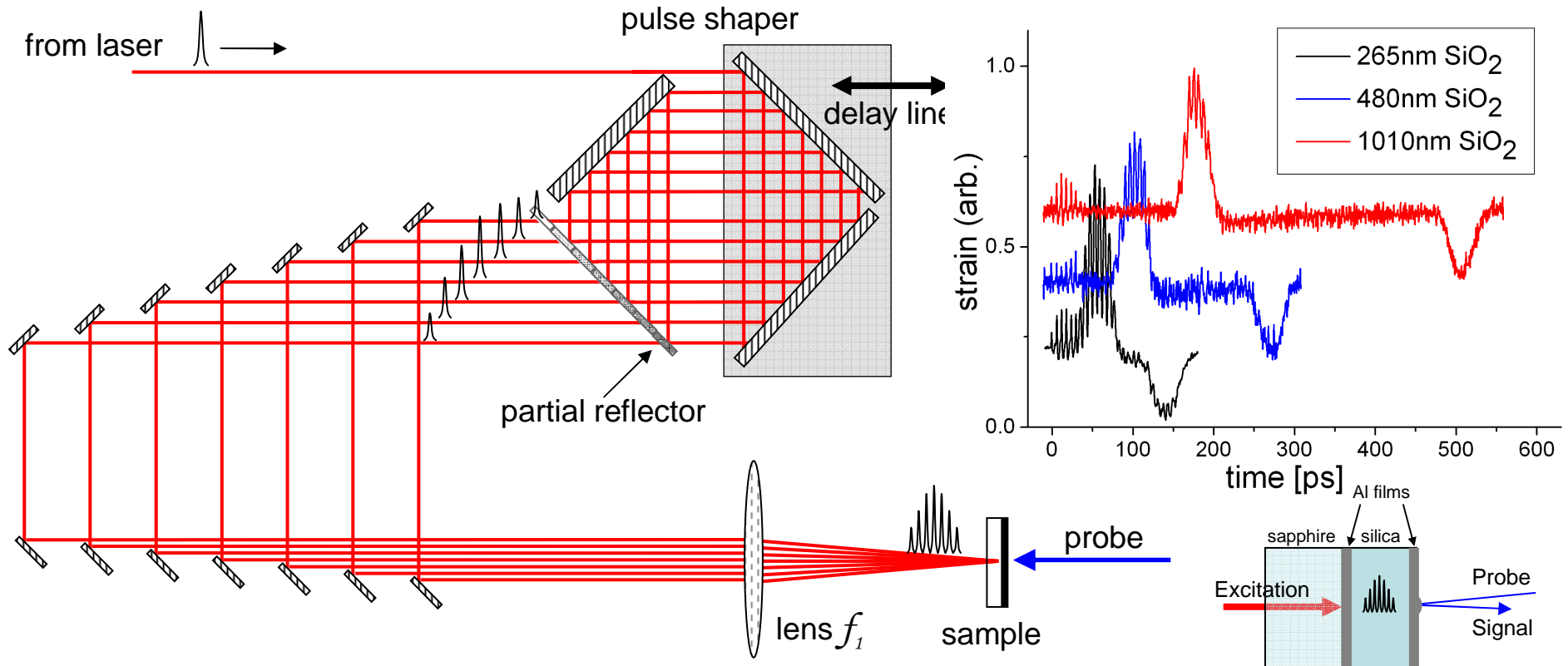


Glass multiple correlation lengths d

Coherent control GHz-THz acoustic waves

“Deathstar” multiple-pulse excitation of acoustic modes
Frequency tunable throughout the Brillouin zone

165 GHz transmission through silica

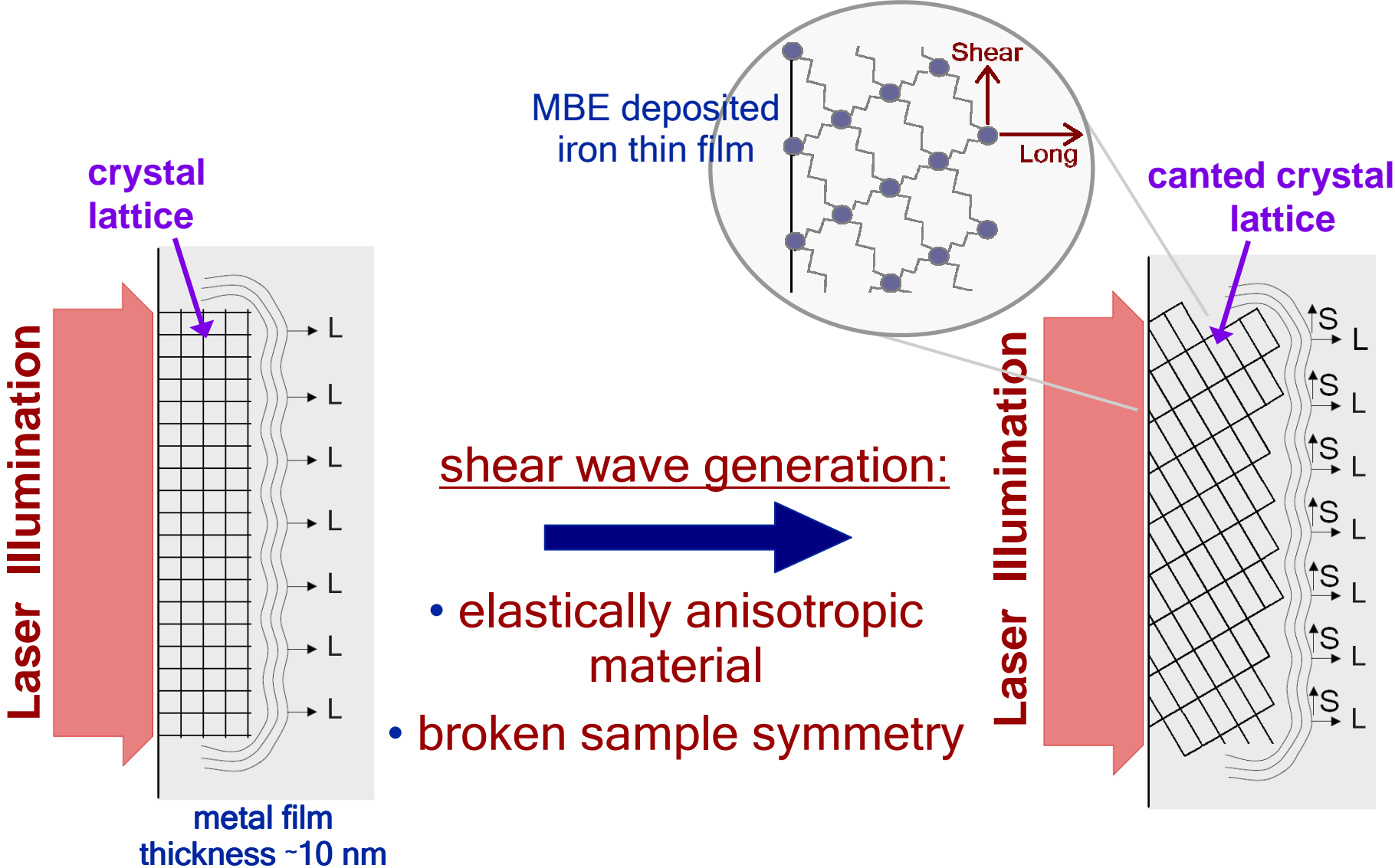


Frequency range 20 MHz – 2 THz

Macroscopic-mesoscopic wavelengths

Detailed study of thermal transport, phononics, nm correlation lengths

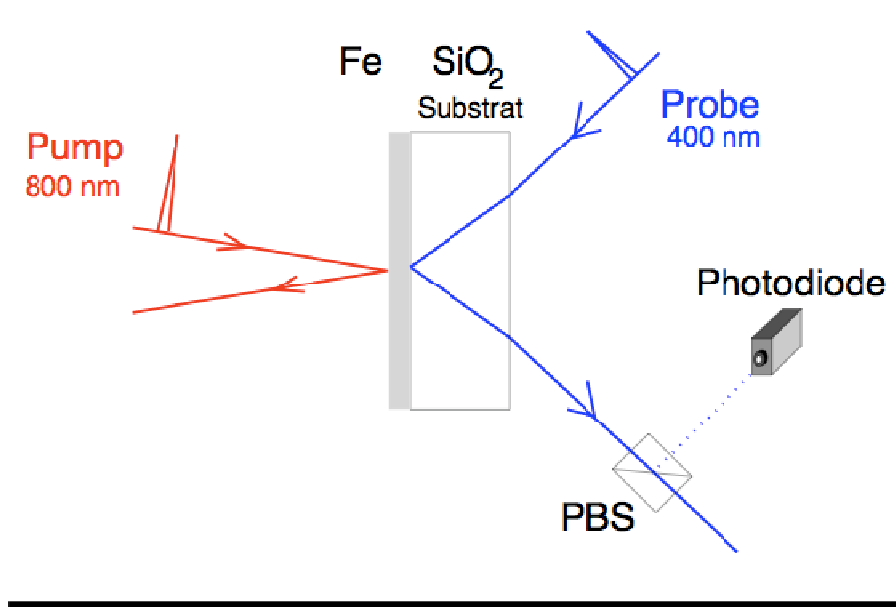
GHz longitudinal & shear wave generation



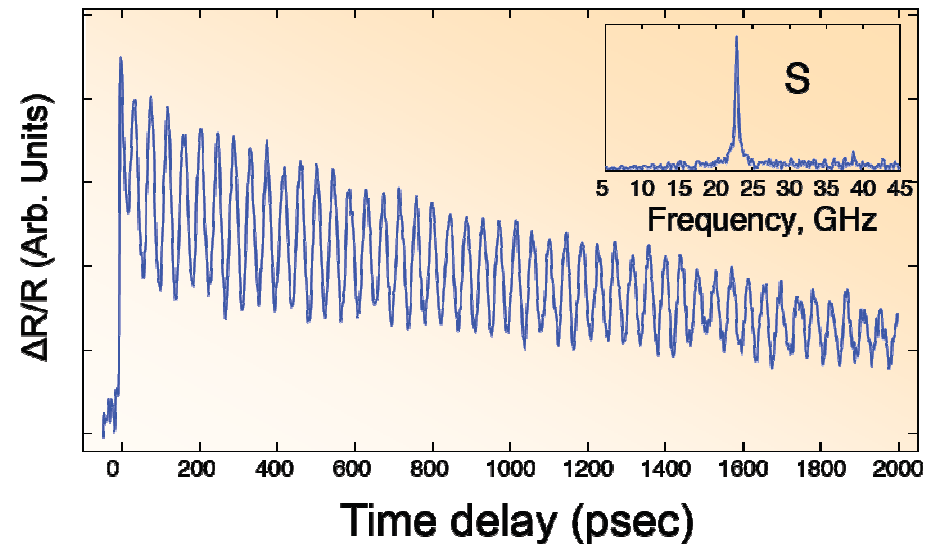
Detection: Depolarized Brillouin scattering

Selects acoustic polarization & frequency

Setup for depolarized Brillouin scattering



Shear wave data from silica glass



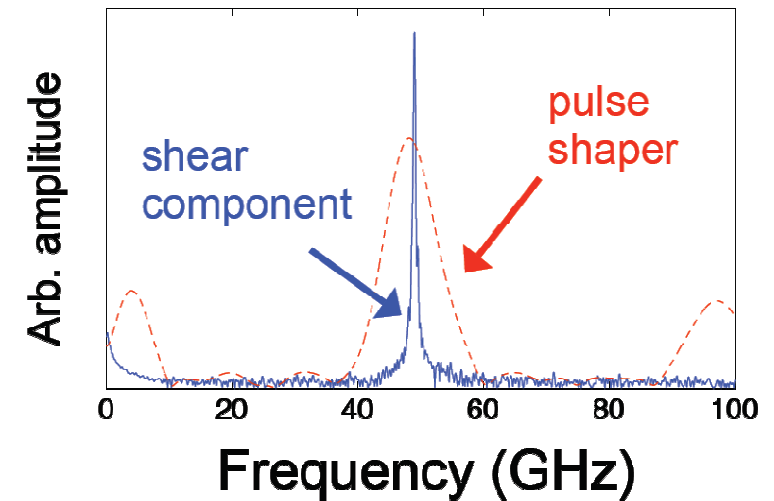
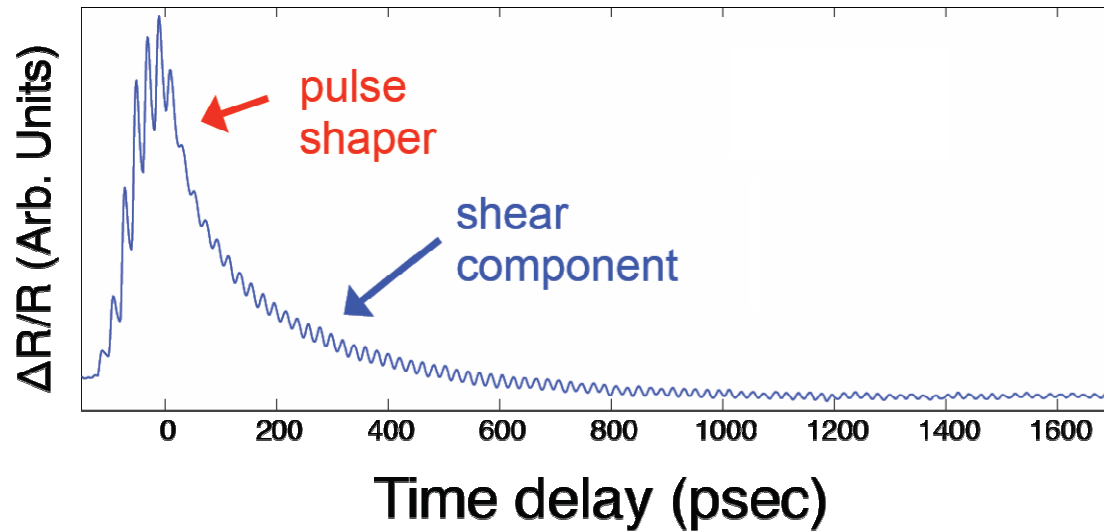
Signal from substrate reveals acoustic wave after propagation through sample

Silica glass or sapphire substrate used for different frequency ranges

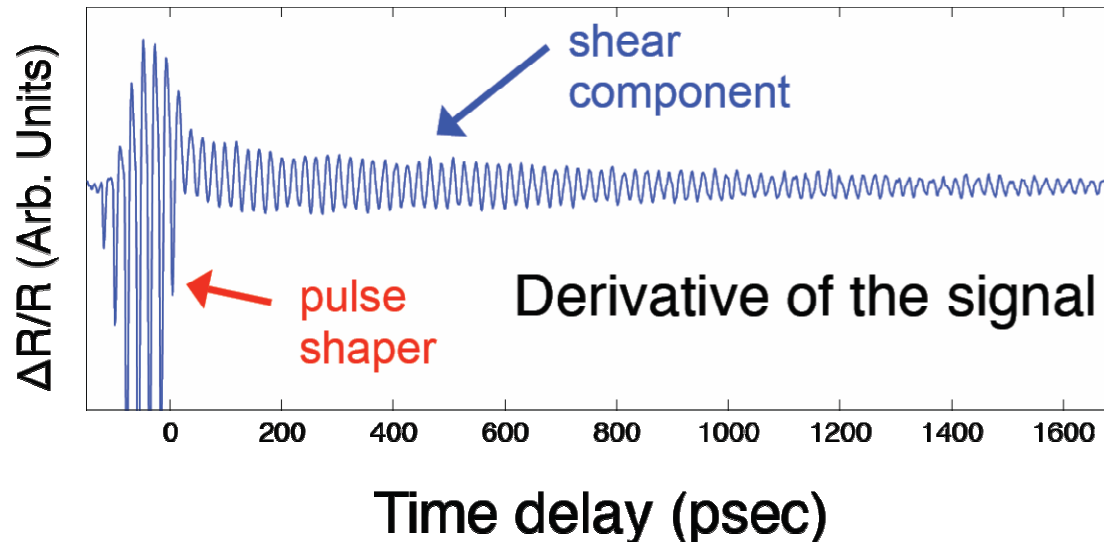
Depolarized Brillouin scattering detection

Deathstar multiple-pulse excitation

Excitation period matches Brillouin frequency



50 GHz shear waves measured
in sapphire substrate



Enhancement of shear
wave spectral brightness

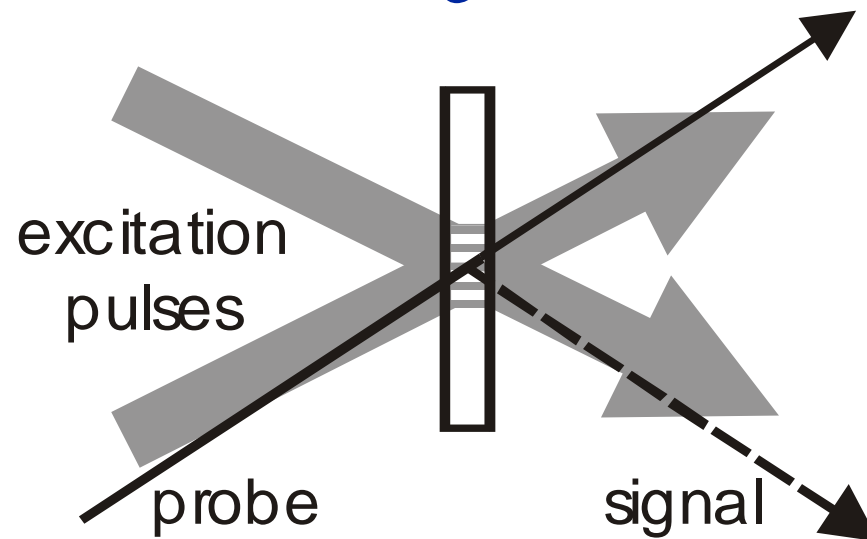
Four-wave mixing and acoustic waves

Acoustic wavevector selected experimentally

Acoustic response driven “impulsively” by short laser pulses

Impulsive stimulated Brillouin & thermal scattering

Real-time observation through time-resolved four-wave mixing

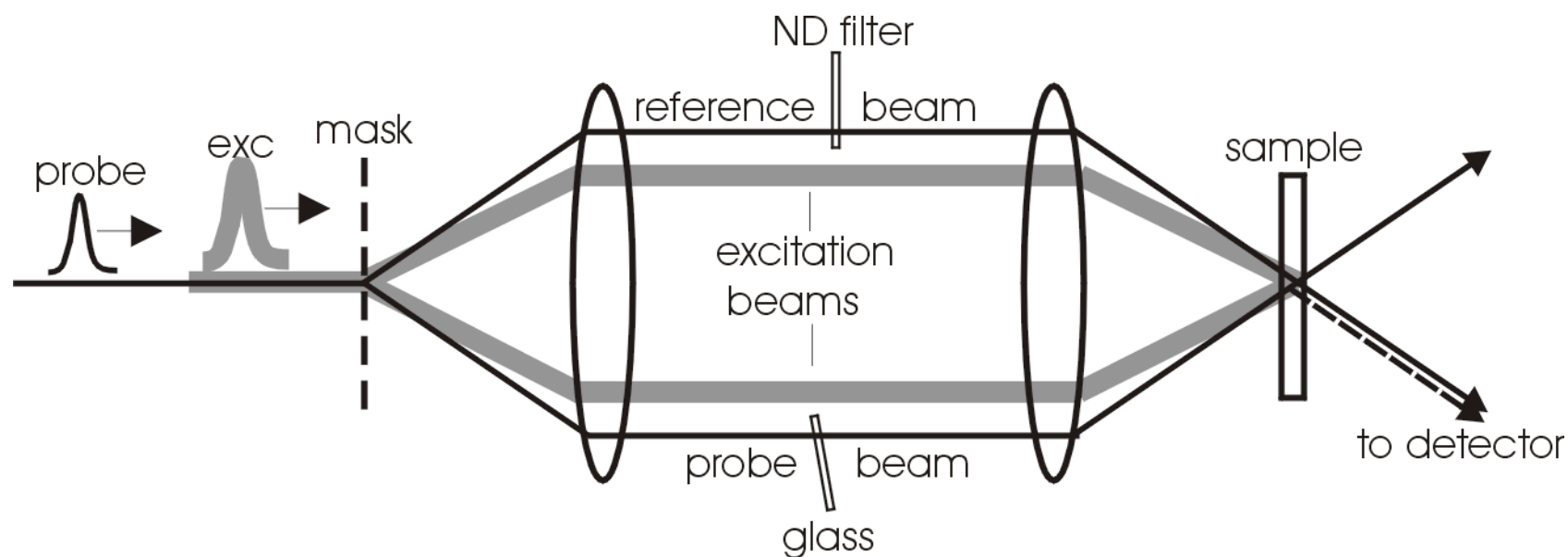


Crossed excitation pulses form interference “grating” pattern
Spatially periodic, temporally “impulsive” driving force exerted

Spatially periodic material response diffracts probe light

Grating wavevector \hat{q} is the phonon wavevector

Heterodyne detection 4-wave mixing setup

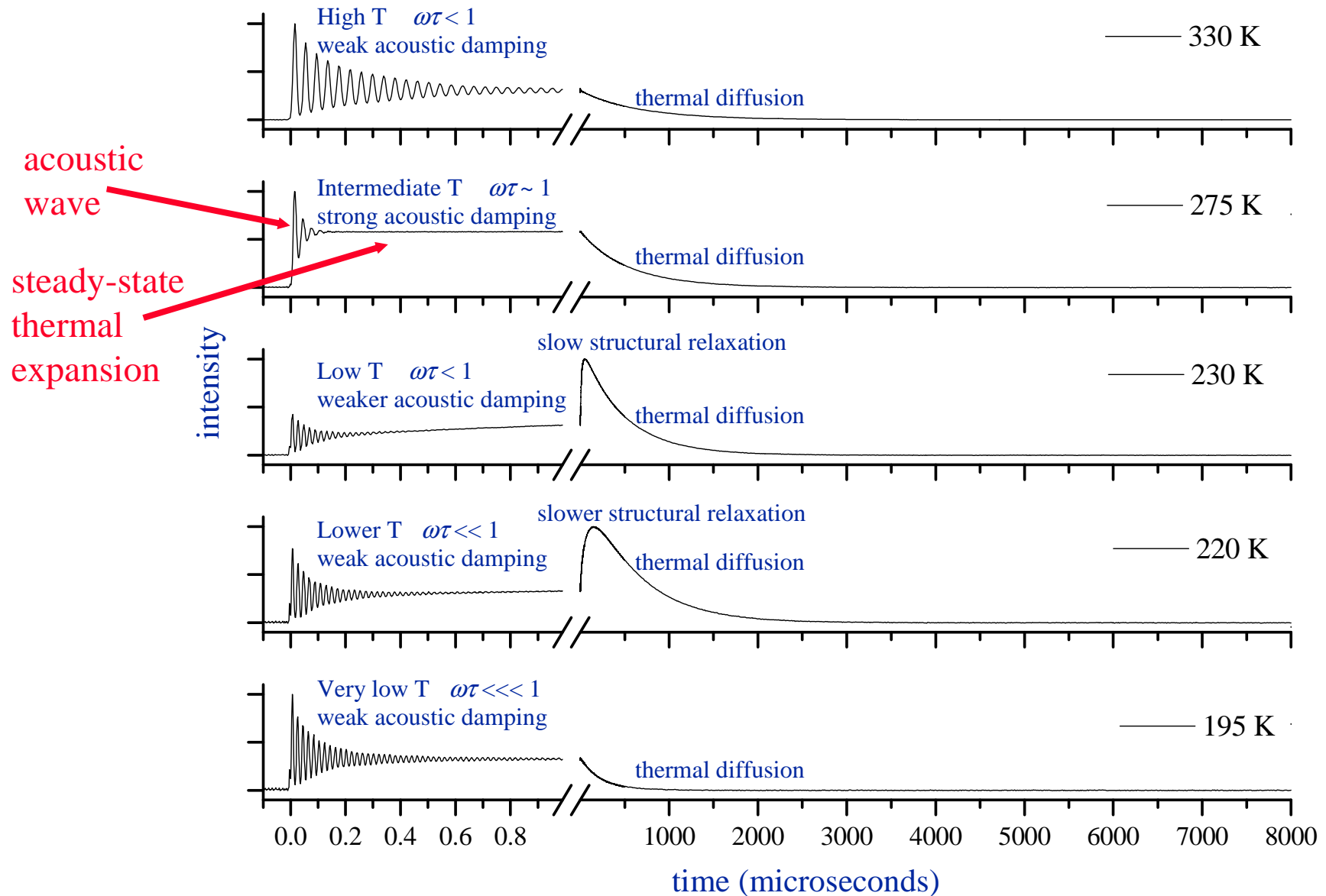


Coherent scattering angle varied for wavevector selection

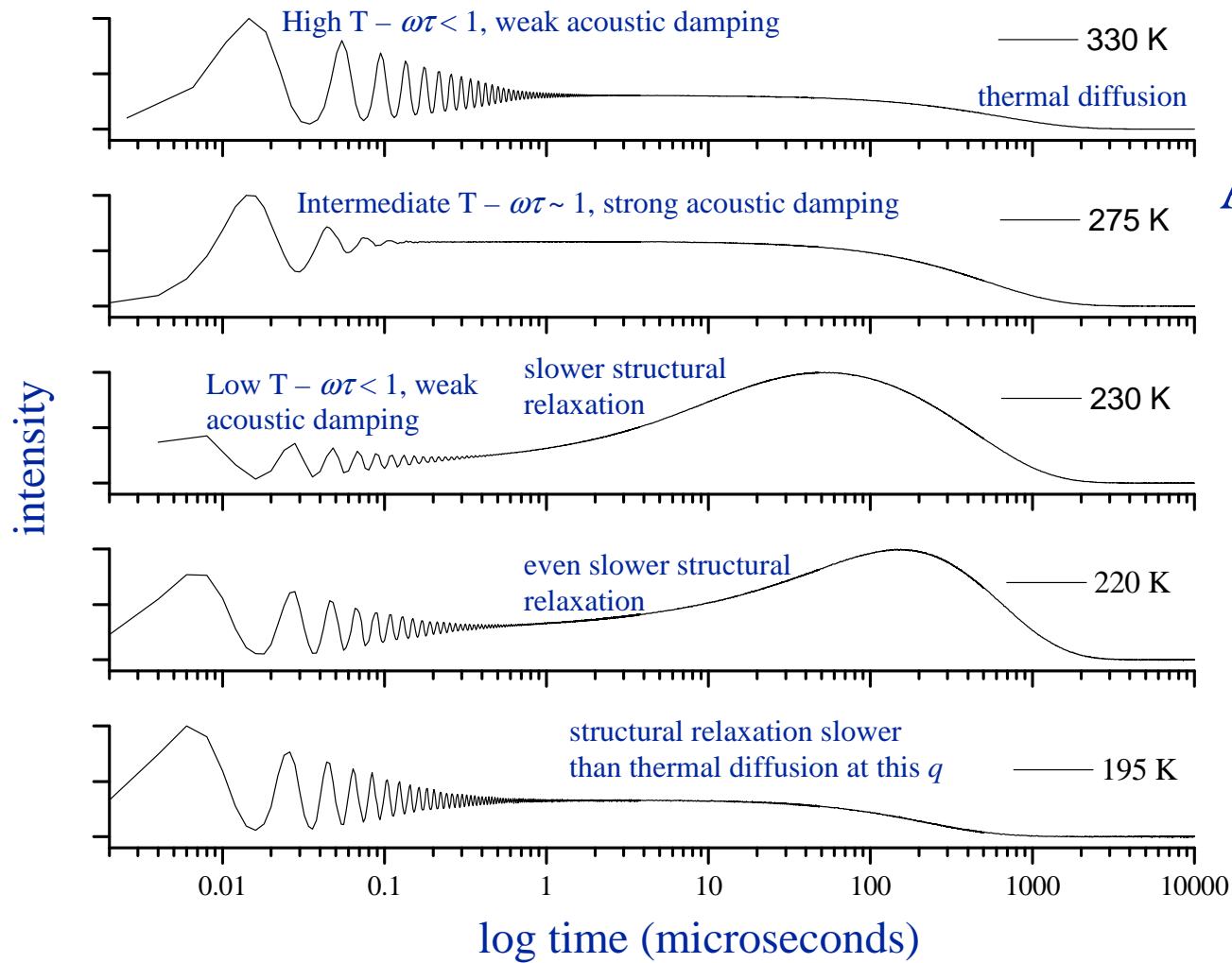
~ 30 MHz – 3 GHz frequency range now reached

ISTS data from glycerol

$q = 0.086 \mu\text{m}^{-1} \leftrightarrow \Lambda = 73 \mu\text{m}$
Acoustic & slower density dynamics



ISTS data from glycerol
 $q=0.086 \mu\text{m}^{-1}$
~7 decades temporal range

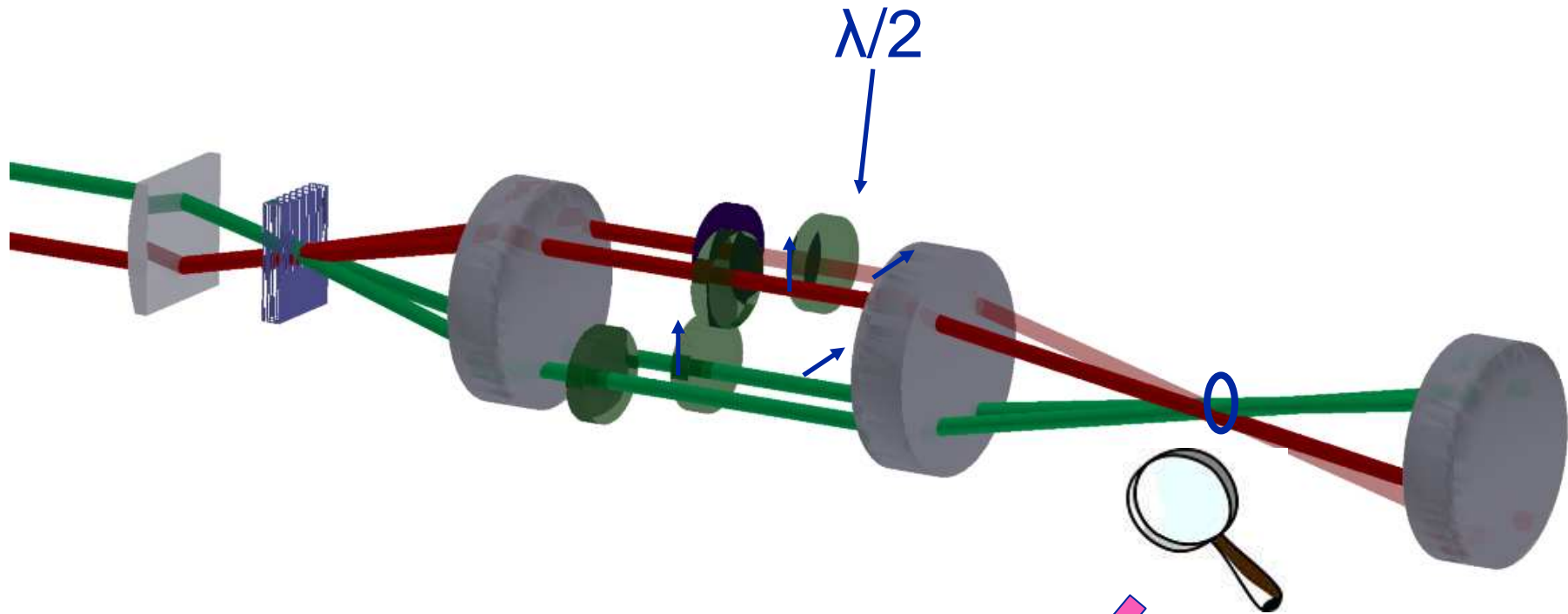


Acoustic signal on ns time scales

Slower structural relaxation on ns- μs time scales

Shear wave generation

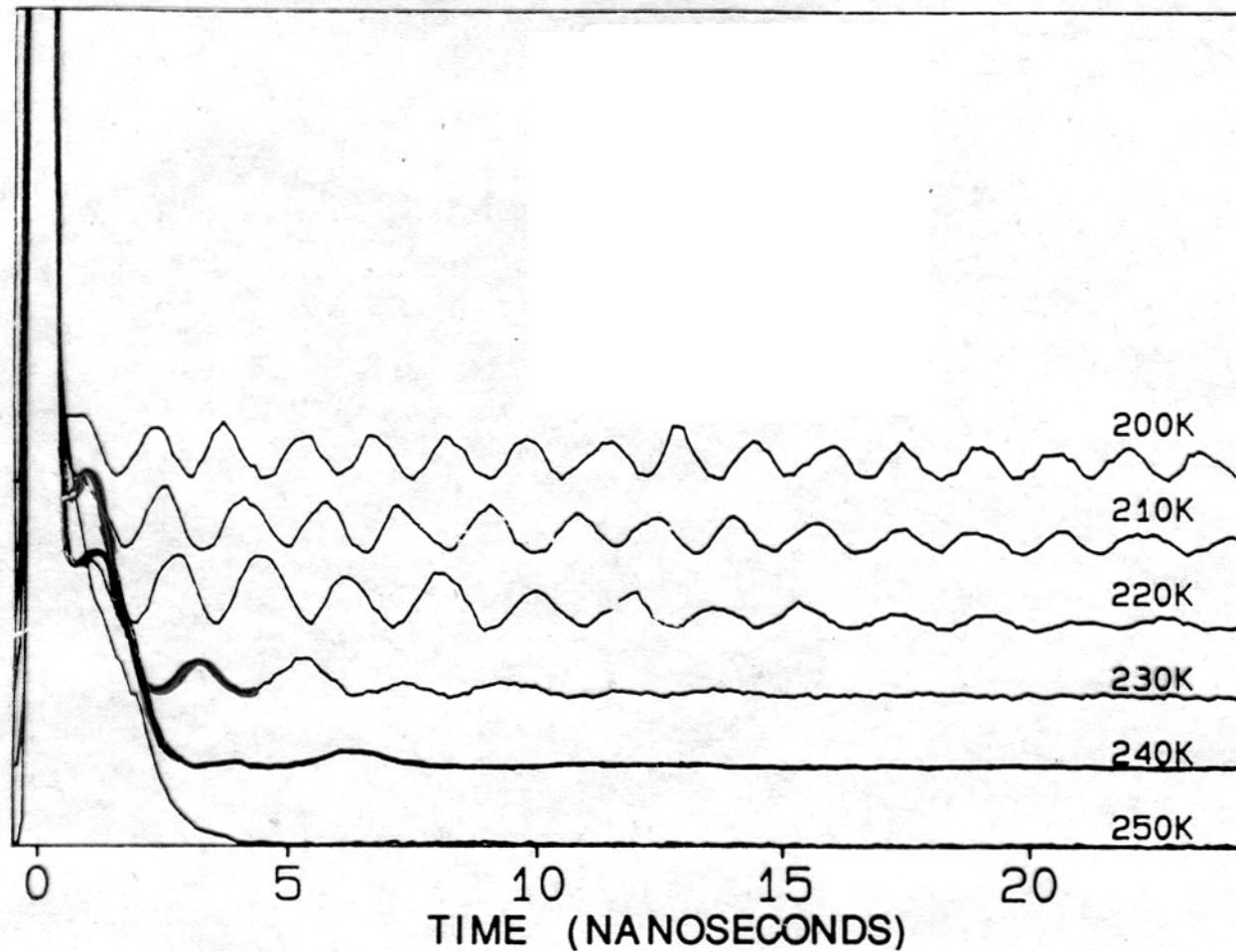
VH excitation pulse polarizations



Shear acoustic waves

Depolarized impulsive stimulated Brillouin scattering (ISBS)

ONSET OF SHEAR ACOUSTIC RESPONSE IN TRIPHENYLPHOSPHITE



Recent results show different longitudinal & shear relaxation dynamics

MHz-GHz acoustic capabilities

Multiple-pulse GHz frequency selection

~ 10-400 GHz longitudinal frequency range

Can be extended to > 1 THz

~ 5-50 GHz shear frequency range

Can be extended to ~ 100 GHz

Christoph Klieber

Crossed-pulse GHz wavevector selection

~ 30-3000 MHz longitudinal frequency range

Can be extended to > 10 GHz

~ 100-1000 MHz shear frequency range

Can be extended to $\sim 50-5000$ MHz

Jeremy Johnson

Picosecond Shear Acoustic Waves in Liquid Glycerol

Christoph Klieber, Thomas Pezeril, Kara Manke, Keith A. Nelson

Department of Chemistry, Massachusetts Institute of Technology

Stephan Andrieu

Laboratoire de Physique des Matériaux UMR7556, Université H. Poincaré / Nancy I

Motivation

Probing high-frequency acoustic responses of liquids

Mapping the frequency dependence of the mechanical response of liquids over as many orders of magnitude as possible

Test first-principles theory and model predictions for supercooled liquids

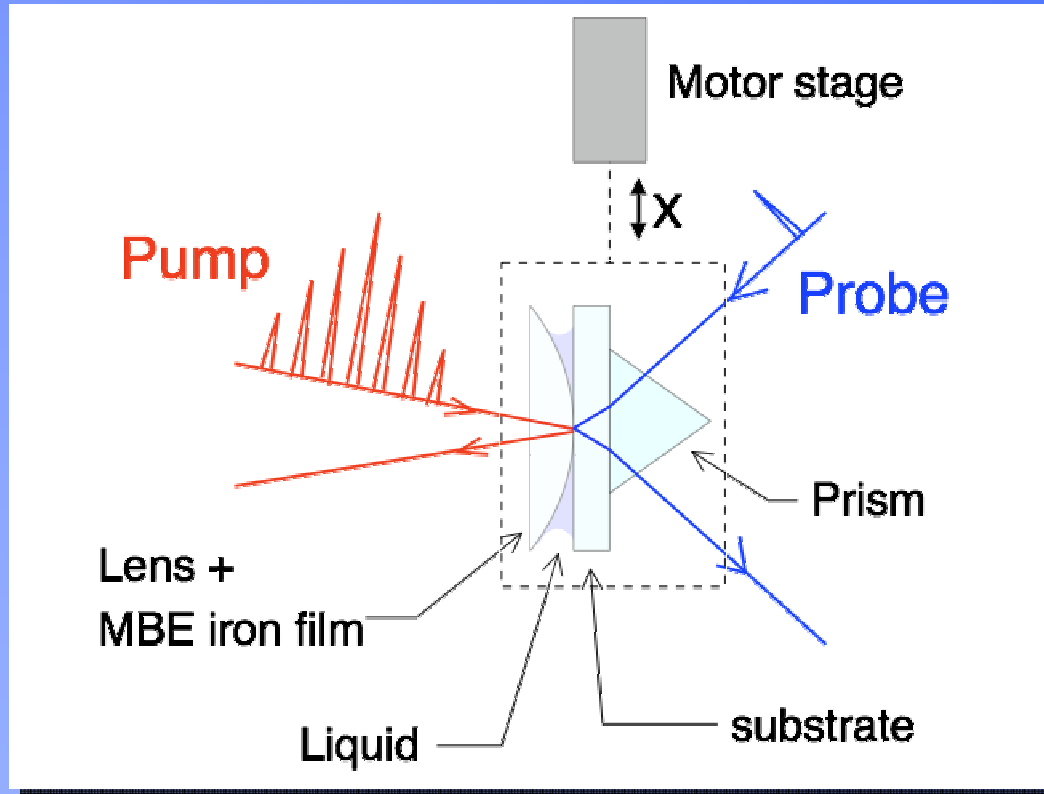
Our Approach

Generation of coherent shear acoustic wave packets

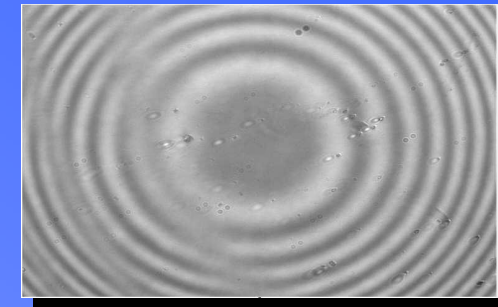
“Death Star” pulse shaper for frequency selectivity and enhancement

Picosecond Brillouin spectroscopy (PBS) analysis

Shear Acoustic Waves in Liquid Glycerol



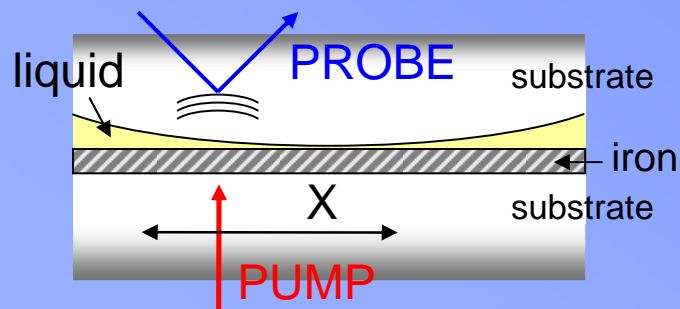
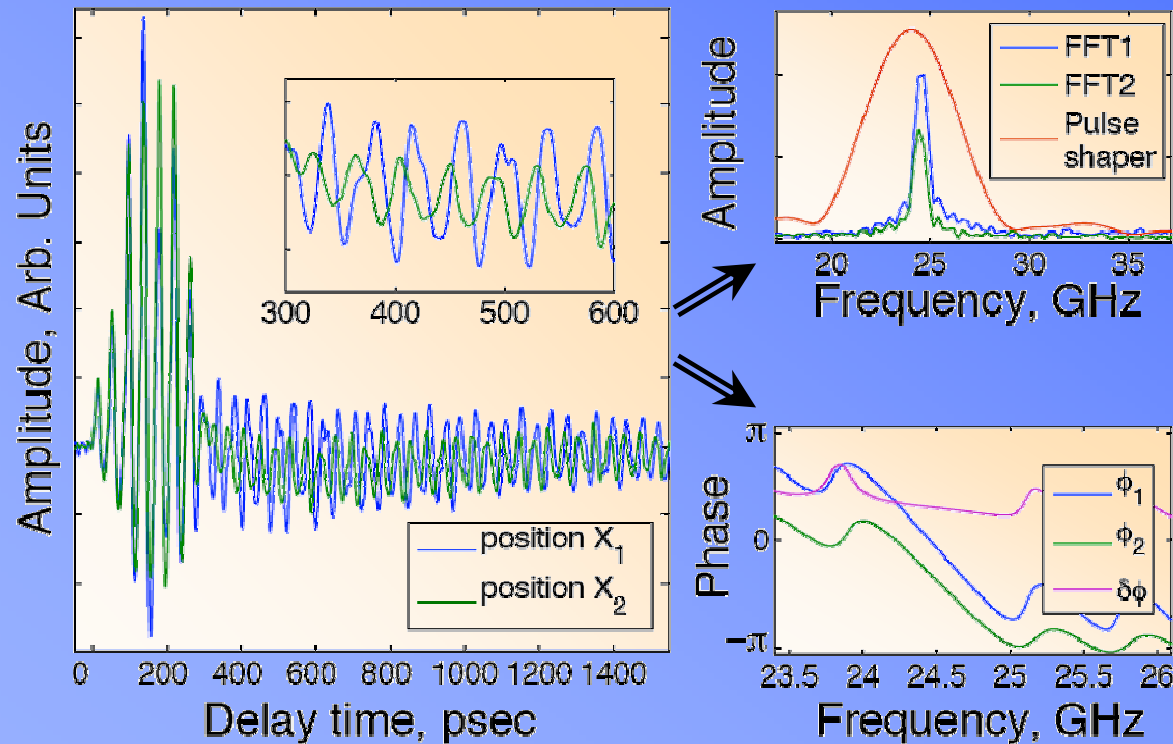
Newton's rings



- Study of thin liquid films of variable thicknesses
- Brillouin frequency tunable between 20/40 GHz and 50/95 GHz with prism
- Either glass or sapphire as a gauge Brillouin medium

Shear Acoustic Waves in Liquid Glycerol

Picosecond Brillouin spectroscopy (PBS)



Brillouin amplitude

$$\sim \exp(-\alpha d)$$

acoustic
attenuation

thickness

The Brillouin amplitude carry out information on the acoustic damping at the Brillouin frequency

Brillouin phase

$$\phi \sim -2\pi\nu_B(d/v)$$

frequency

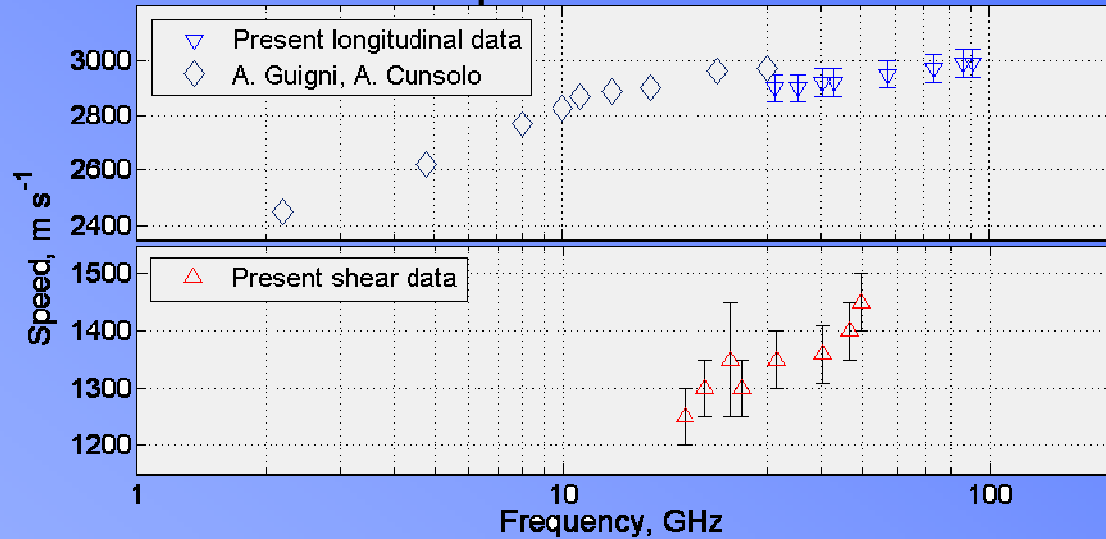
thickness

speed

The Brillouin phase is proportional to the time of flight through the liquid film

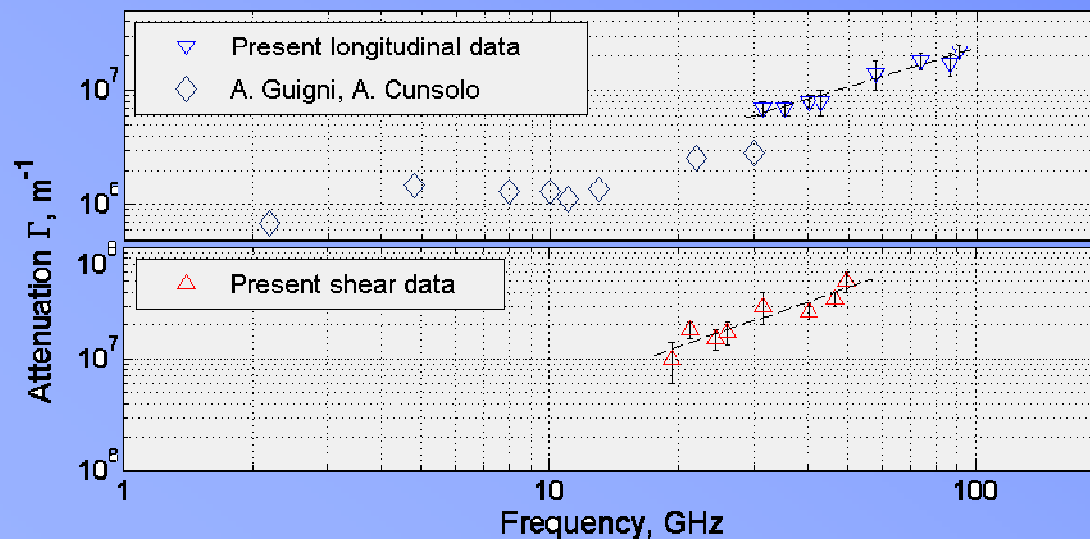
Glycerol at Room Temperature

Speed of Sound



- Longitudinal speed of sound has reached its infinite-frequency value
- Shear frequency range overlaps with the high-frequency edge of alpha relaxation

Attenuation



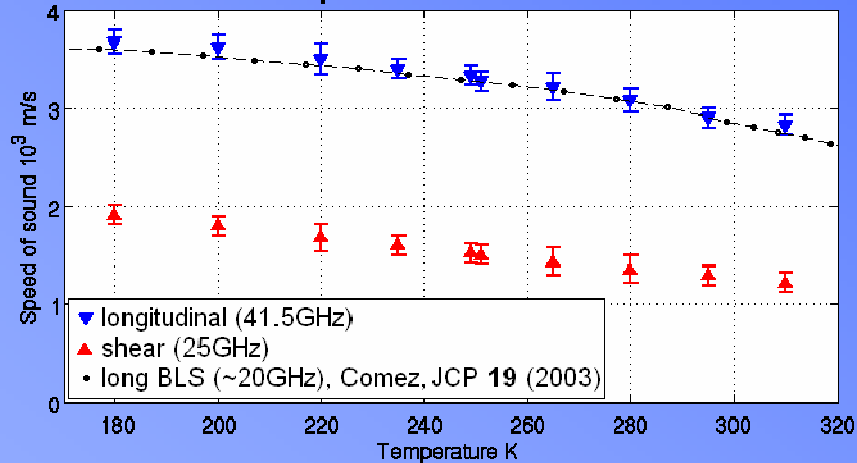
- Close to linear frequency dependence of attenuation

$$\eta_s = \frac{3\alpha_s \rho v_s^3}{2\omega^2}$$

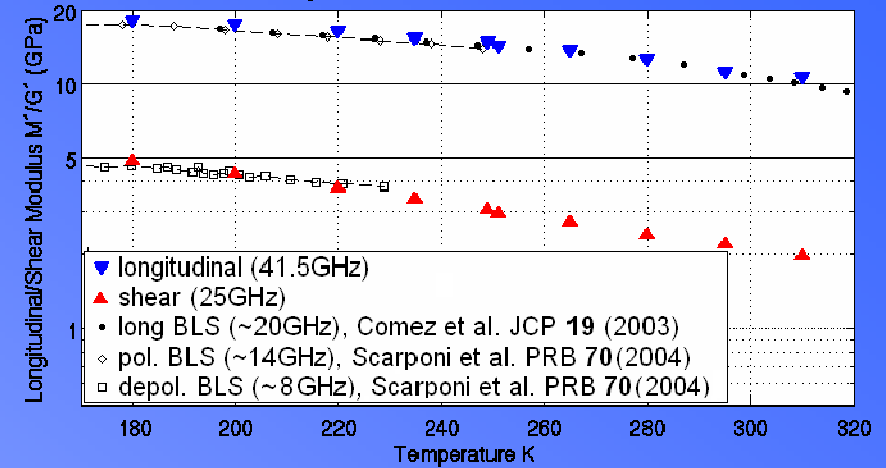
- This indicates a frequency dependent shear viscosity

Temperature Dependent Acoustic Moduli of Glycerol

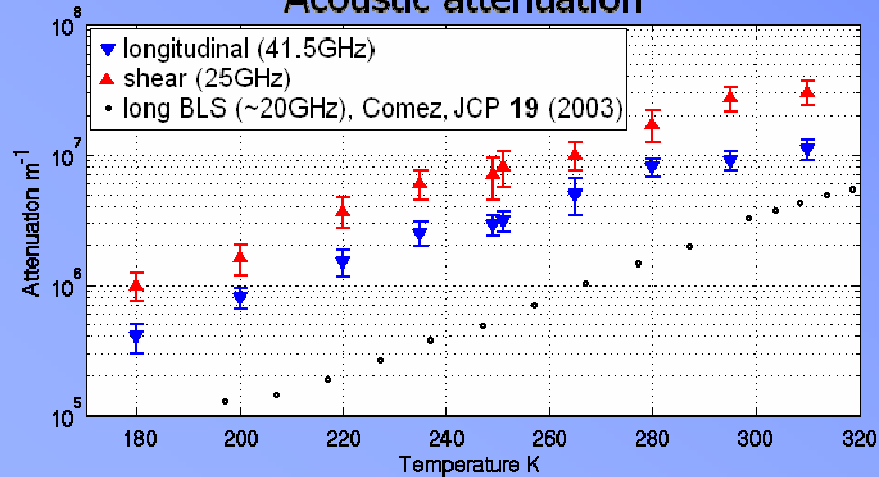
Speed of sound



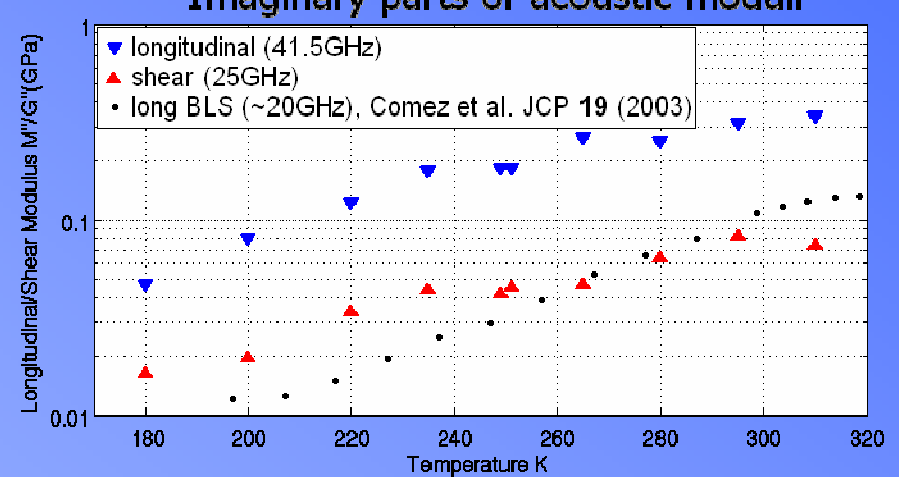
Real parts of acoustic moduli



Acoustic attenuation



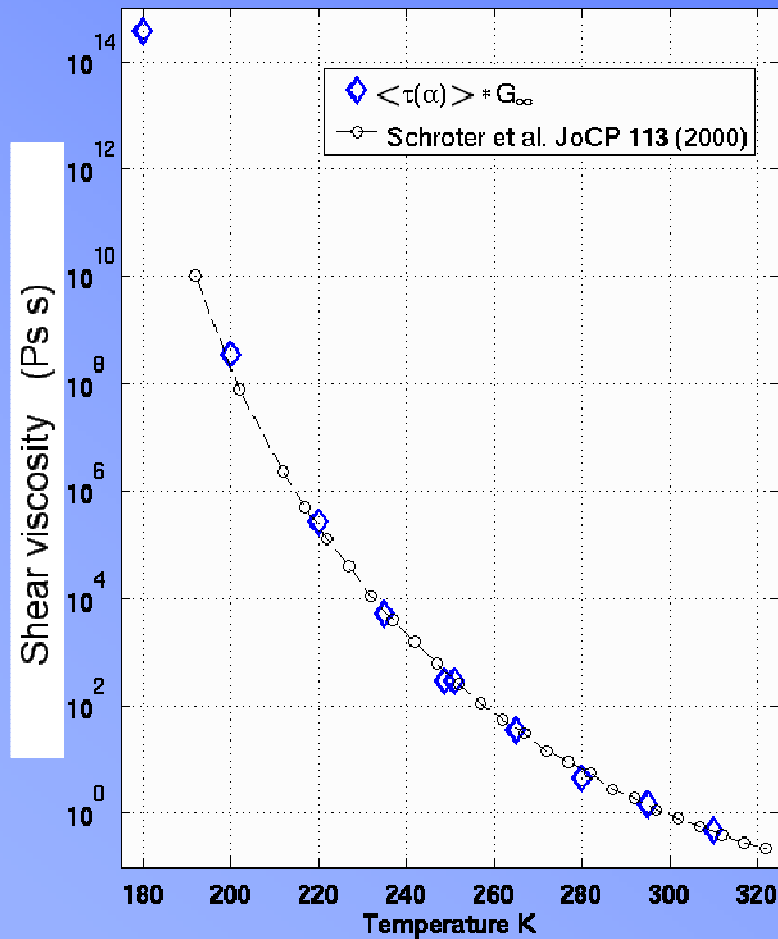
Imaginary parts of acoustic moduli



$$\hat{v}(\omega) = \frac{\omega}{\hat{q}(\omega)} \approx v'(\omega) - i \frac{\alpha(\omega) \cdot v'(\omega)^2}{\omega}$$

$$\hat{M}(\omega) = \rho \cdot \hat{v}(\omega)^2$$

Instant. Shear Modulus and Static Shear Viscosity



➤ Measurement of the high frequency limits of the elastic moduli K_∞ / G_∞ , even far above the glass transition temperature

➤ Instantaneous shear modulus G_∞ can be used to estimate the shear viscosity through the well-known Maxwell relation:

$$\eta_S = G_\infty \cdot \langle \tau(\alpha) \rangle_{TA}$$

Conclusion

- Robust measurement applicable to many liquid and soft matter samples
- Measurement of longitudinal and shear acoustic properties of liquid Glycerol at GHz frequencies

Outlook

Measurements at higher frequencies

Measurements over larger temperature interval

Other liquids, tests of first-principles theory and model predictions for supercooled liquids

More shear measurements of water

Coherent MHz Longitudinal and Shear Acoustic Phonons in Glass Forming Liquids

Jeremy A. Johnson, Darius H. Torchinsky, Keith A. Nelson

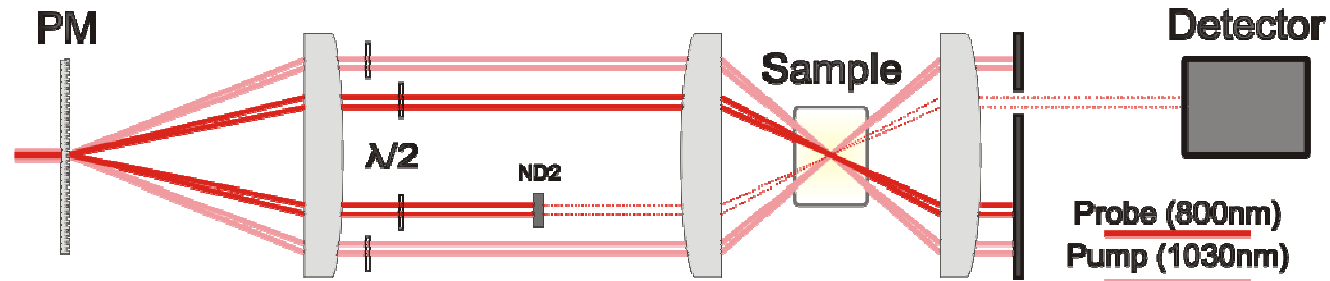
Fragility of Viscous Liquids: Cause(s) and Consequences

8 Oct 2008

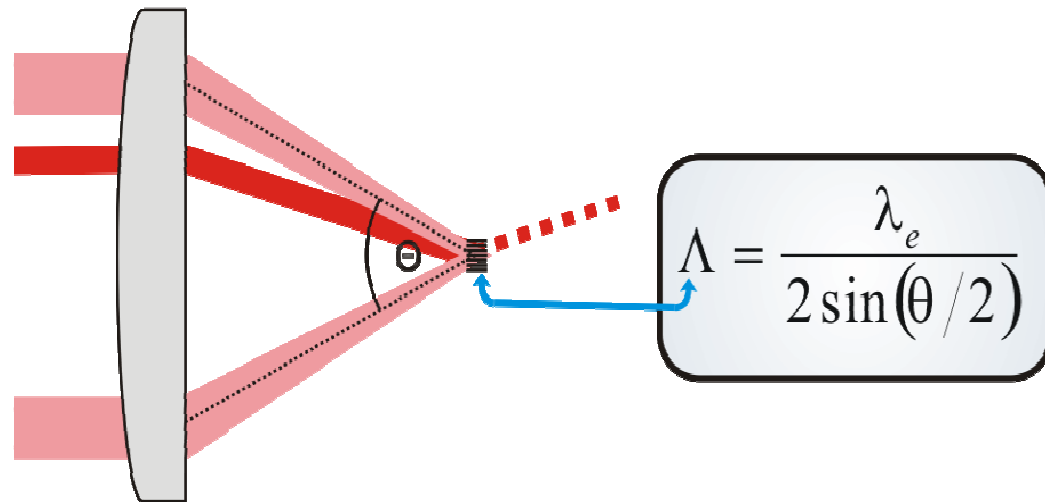
Outline

- Experimental
 - ISTS (longitudinal)
 - ISBS (shear and longitudinal)
- Results and Tests of Theory
 - Shoving Model (shear)
 - Poisson Ratio (shear and longitudinal)
 - TPP (shear vs. longitudinal)
 - DC704 (longitudinal)

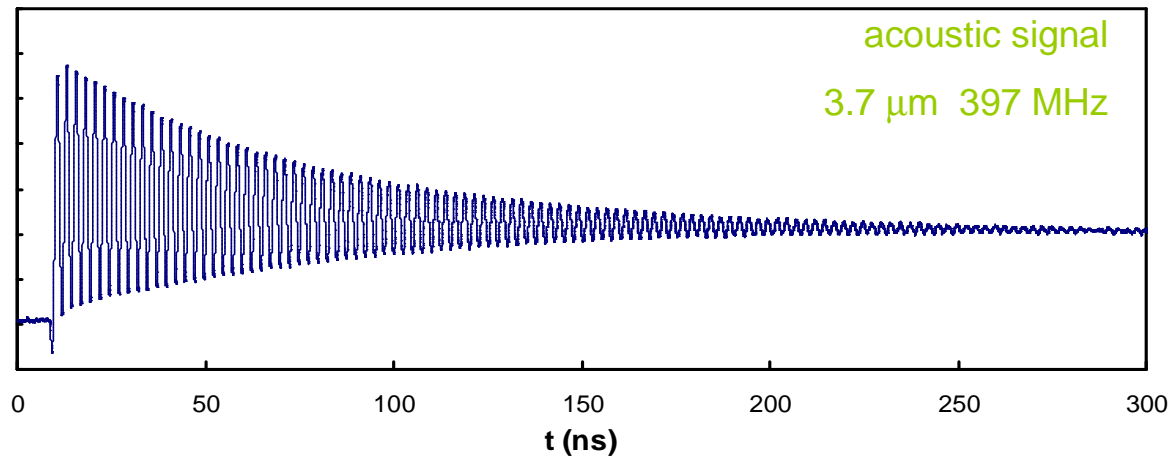
Impulsive Stimulated Scattering



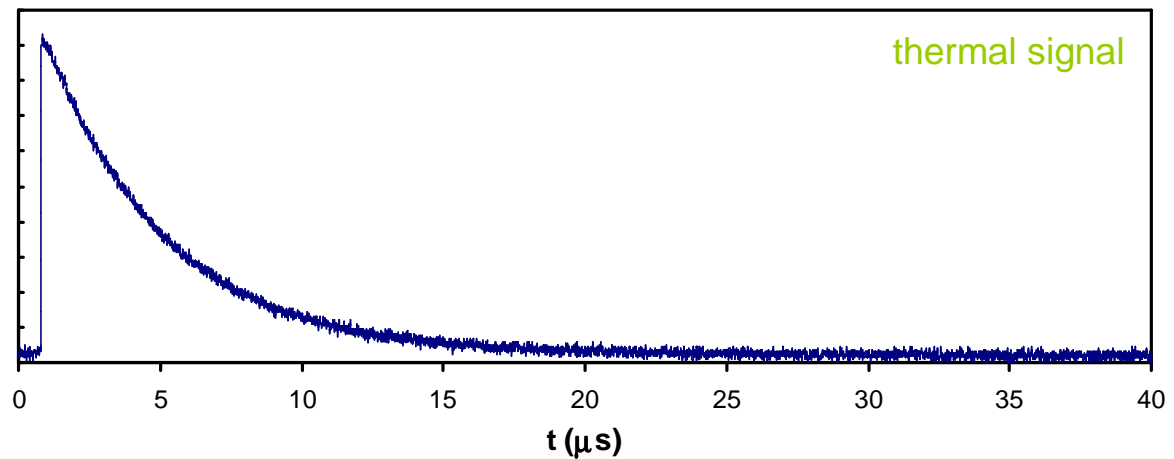
- Crossed laser pulses generate counter-propagating acoustic waves with wavelength Λ
- Probe beam diffracts off of relaxing region and time dependent relaxation is observed



ISTS Signal



- Short times gives measurement of acoustic frequency and damping rate



- Longer times gives measurement of thermal decay rate

ISTS Signal

- With acoustic frequency and damping rate, we can determine the frequency dependent complex modulus

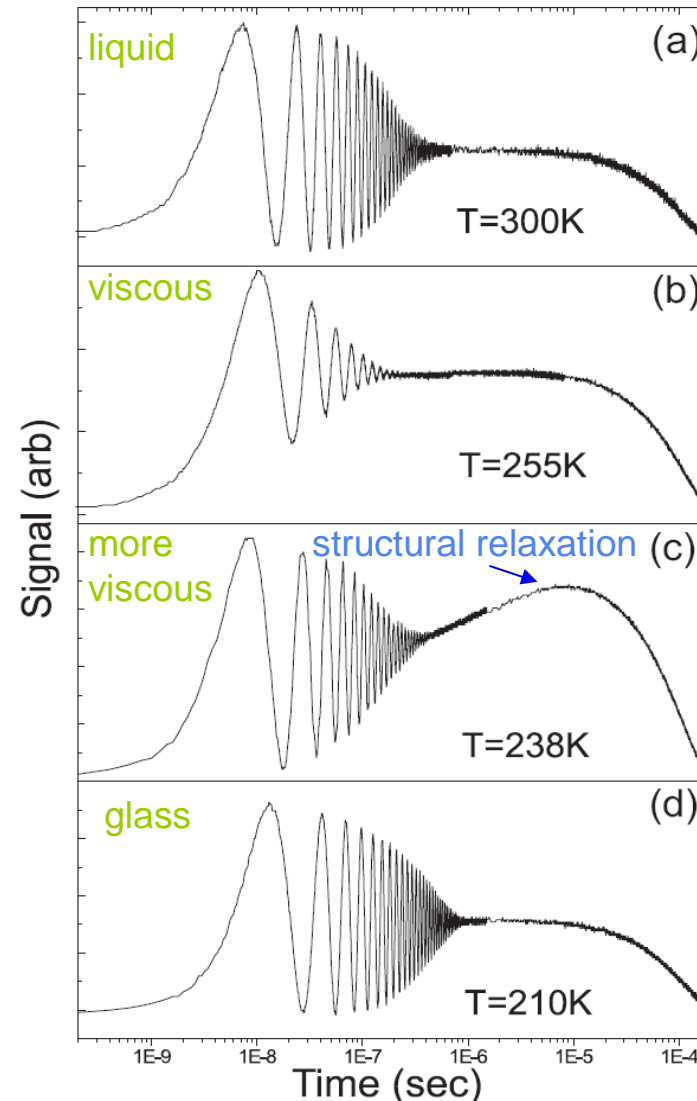
$$M^*(\omega) = M'(\omega) + iM''(\omega)$$

$$M'(\omega_A) = \rho \frac{\omega_A^2 - \Gamma_A^2}{q^2}$$

$$M''(\omega_A) = \rho \frac{2\omega_A \Gamma_A}{q^2}$$

- Slow rise allows direct time domain measurement of structural relaxation (α -relaxation)

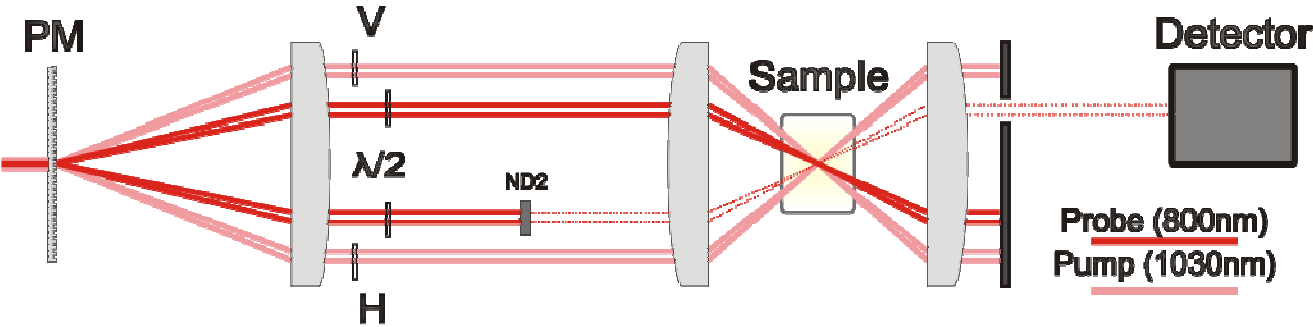
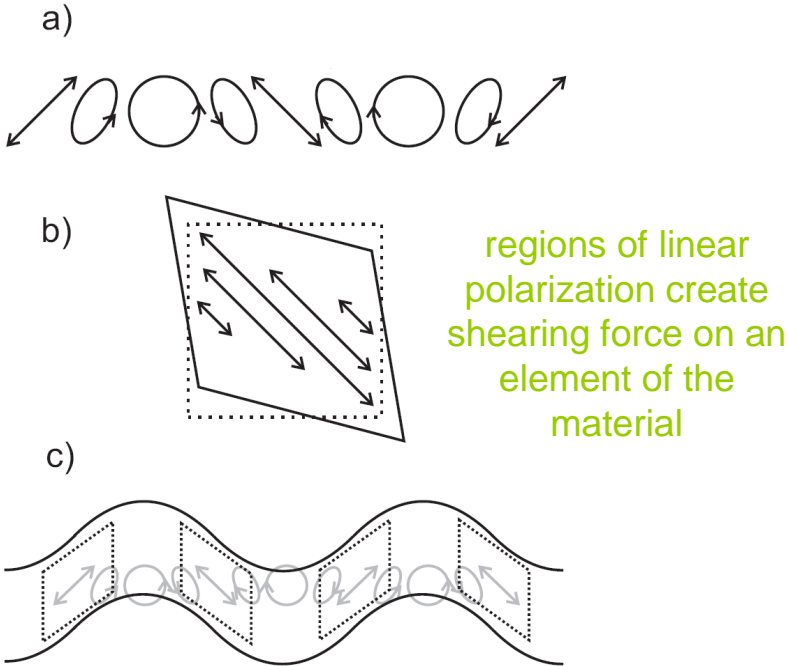
$$e^{-(t/\tau_{KWW})^{\beta_{KWW}}}$$



Longitudinal acoustic signal from the glass former DC704 with an acoustic wavelength of $38.1\mu\text{m}$ as the sample is cooled.

Depolarized ISBS

- Crossed laser pulses with perpendicular polarizations generate counter-propagating shear acoustic waves
- Probe beam is depolarized as it diffracts off of the shear acoustic waves



Shear ISBS

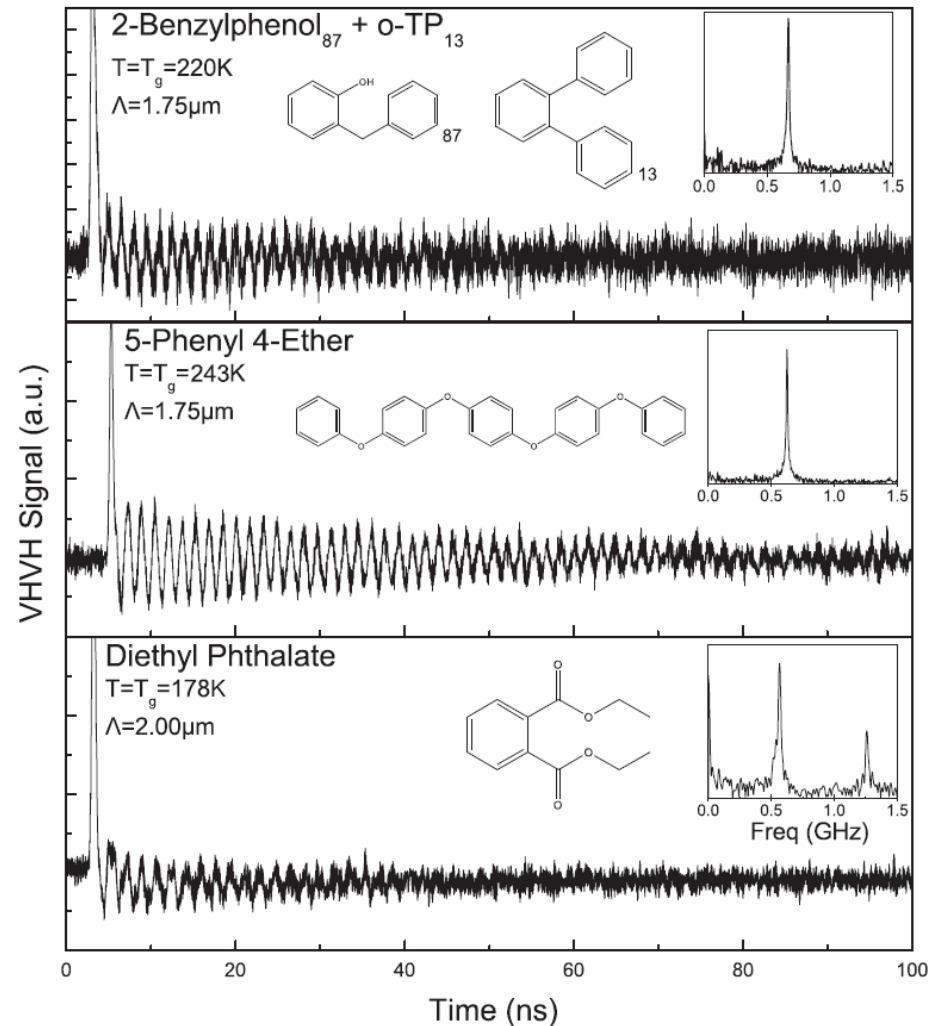
- With shear acoustic frequency and damping rate, we can determine the frequency dependent complex shear modulus

$$G^*(\omega) = G'(\omega) + iG''(\omega)$$

$$G'(\omega_s) = \rho \frac{\omega_s^2 - \Gamma_s^2}{q^2}$$

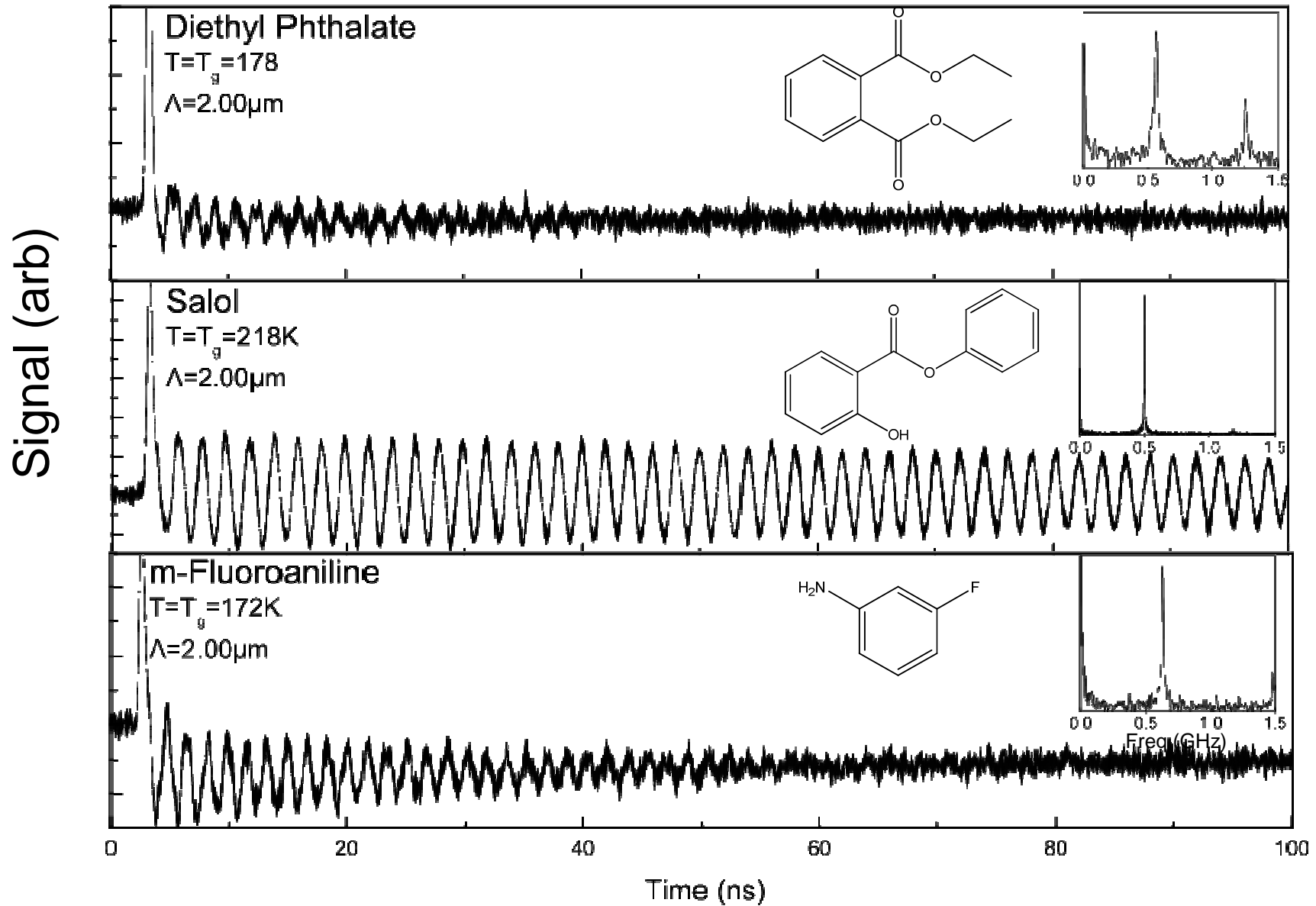
$$G''(\omega_s) = \rho \frac{2\omega_s \Gamma_s}{q^2}$$

- Because there is no absorption, there are no direct structural relaxation or thermal features in the data

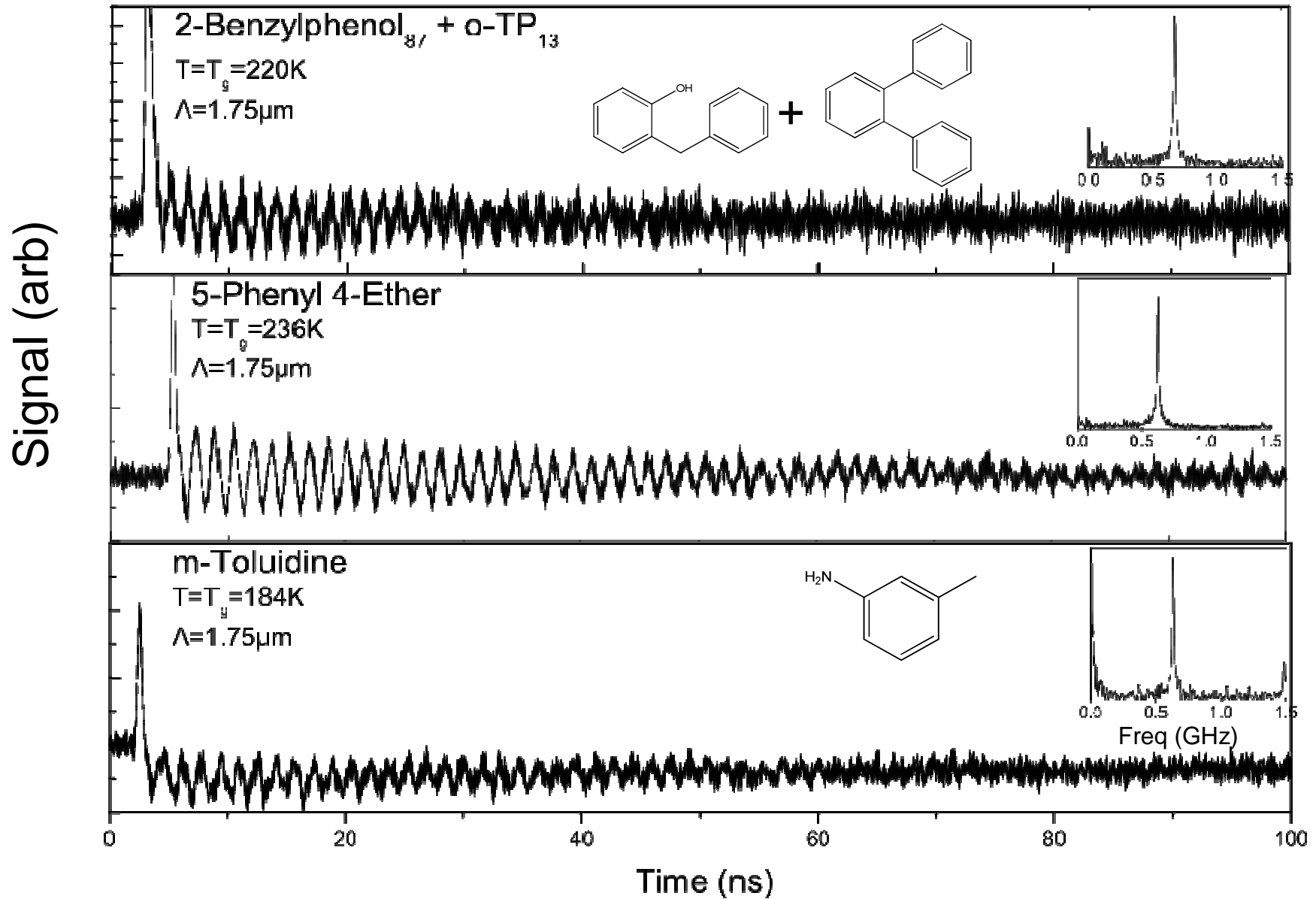


Shear waves in 2-benzylphenol(87%)/o-terphenyl(13%), 5-phenyl 4-ether, and diethylphthalate at their respective T_g. Insets show the Fourier spectrum on the GHz scale

Shear Wave Gallery



Shear Wave Gallery



Outline

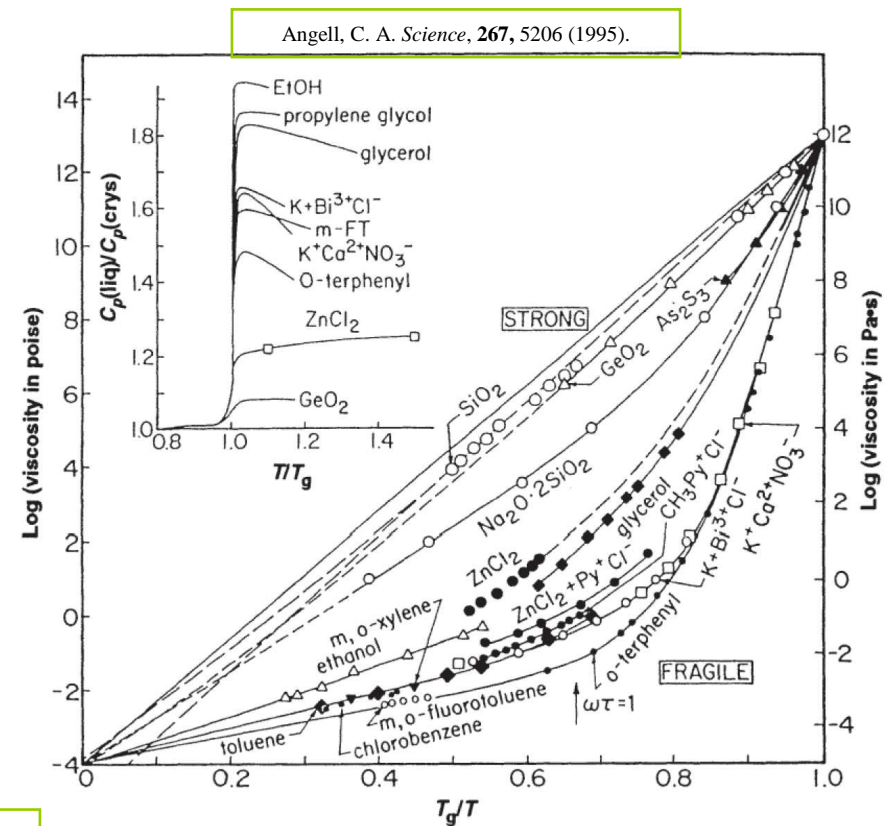
- Experimental
 - ISTS (longitudinal)
 - ISBS (shear and longitudinal)
- Results and Tests of Theory
 - **Shoving Model (shear)**
 - Poisson Ratio (shear and longitudinal)
 - TPP (shear vs. longitudinal)
 - DC704 (longitudinal)

Shoving Model

$$\tau(T) = \tau_0 \exp\left(\frac{\Delta E(T)}{k_B T}\right) \quad \text{or} \quad \eta(T) = \eta_0 \exp\left(\frac{\Delta E(T)}{k_B T}\right)$$

- relaxation depends on rearranging region and surrounding liquid
 - strong short range repulsion
 - elastic response in surroundings
- shoving work depends on infinite frequency elastic moduli: bulk (K_∞) and shear (G_∞)
- G_∞ controls relaxation

Dyre *et al. Phys. Rev. B* **53**, 2171-2174 (1996).

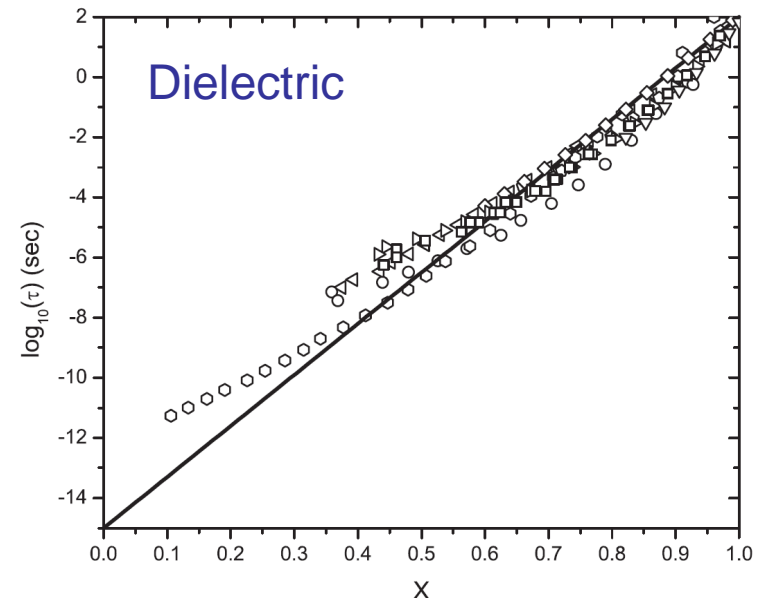
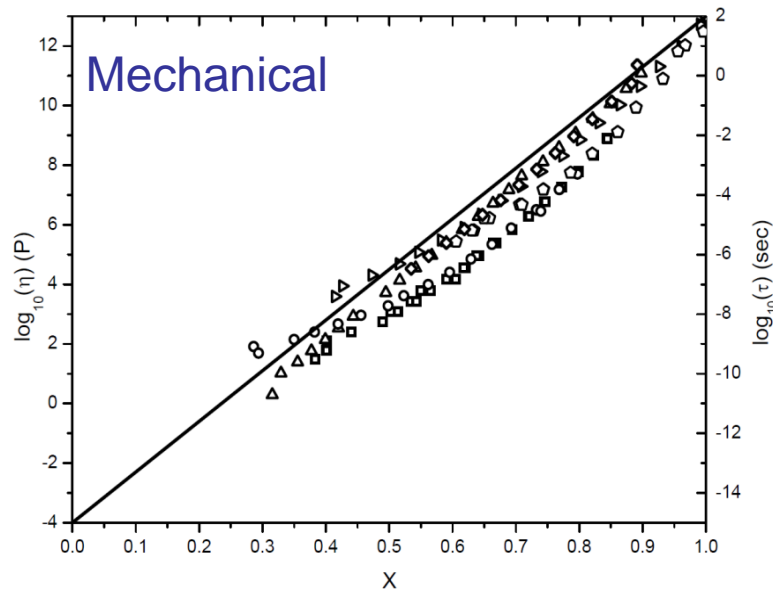


Direct Test of Shoving Model

$$\tau(T) = \tau_0 \exp\left(\frac{G_\infty(T)V_c}{k_B T}\right)$$

$$V_c = \frac{2}{3} \frac{(\Delta V)^2}{V}$$

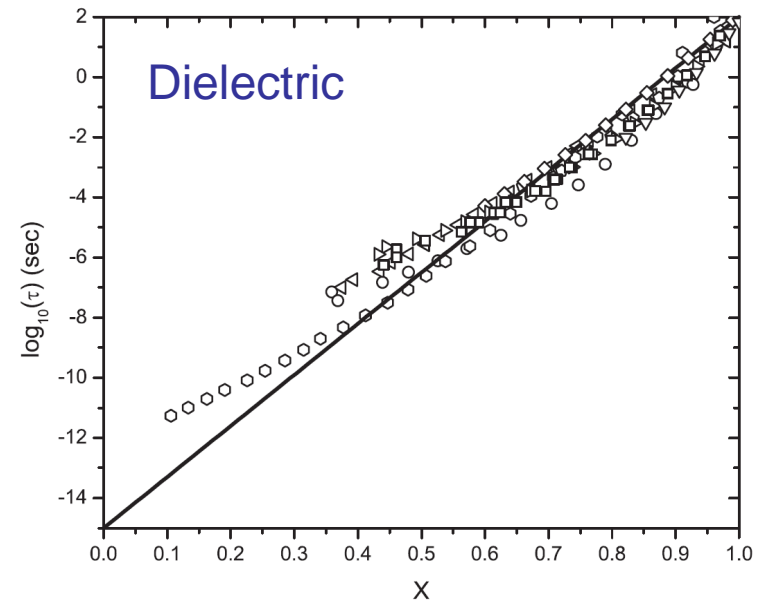
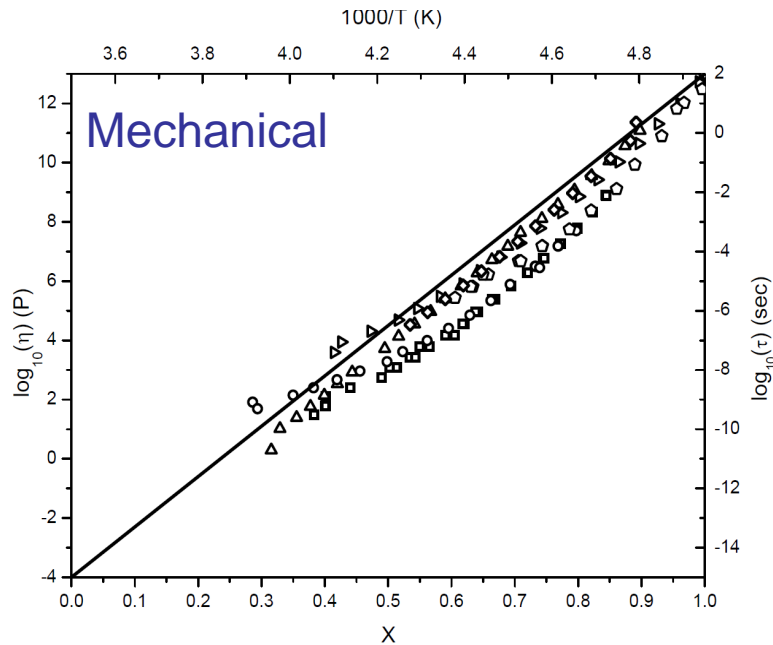
$$X = \frac{G_\infty(T)T_g}{G_\infty(T_g)T}$$



These results support to the notion that the dynamics of the glass transition are governed by the evolution of the shear modulus.

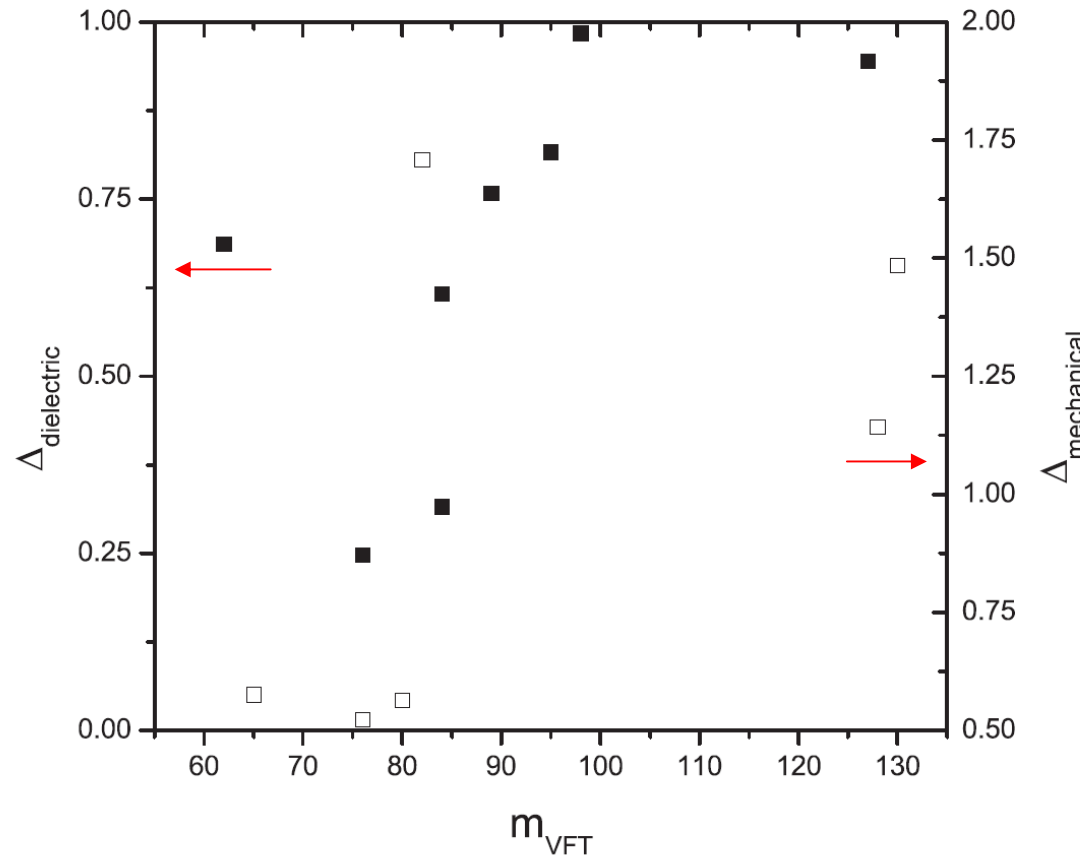
Direct Test of Shoving Model

$$\tau(T) = \tau_0 \exp\left(\frac{G_\infty(T)V_c}{k_B T}\right) \quad V_c = \frac{2}{3} \frac{(\Delta V)^2}{V} \quad X = \frac{G_\infty(T)T_g}{G_\infty(T_g)T}$$



These results support to the notion that the dynamics of the glass transition are governed by the evolution of the shear modulus.

Direct Test of Shoving Model



The root mean square deviation quantifies the amount of departure from the shoving model predicted behavior.

Deviation from the dielectric relaxation data suggests a trend of increasing deviation with increasing fragility.

A similar trend in the mechanical relaxation data is not as clear.

$$\Delta = \sqrt{\sum ((17X_{obs} - 15) - \log_{10}(\tau))^2 / N}$$

Outline

- Experimental
 - ISTS (longitudinal)
 - ISBS (shear and longitudinal)
- Results and Tests of Theory
 - Shoving Model (shear)
 - Poisson Ratio (shear and longitudinal)
 - TPP (shear vs. longitudinal)
 - DC704 (longitudinal)

Poisson Ratio Prediction

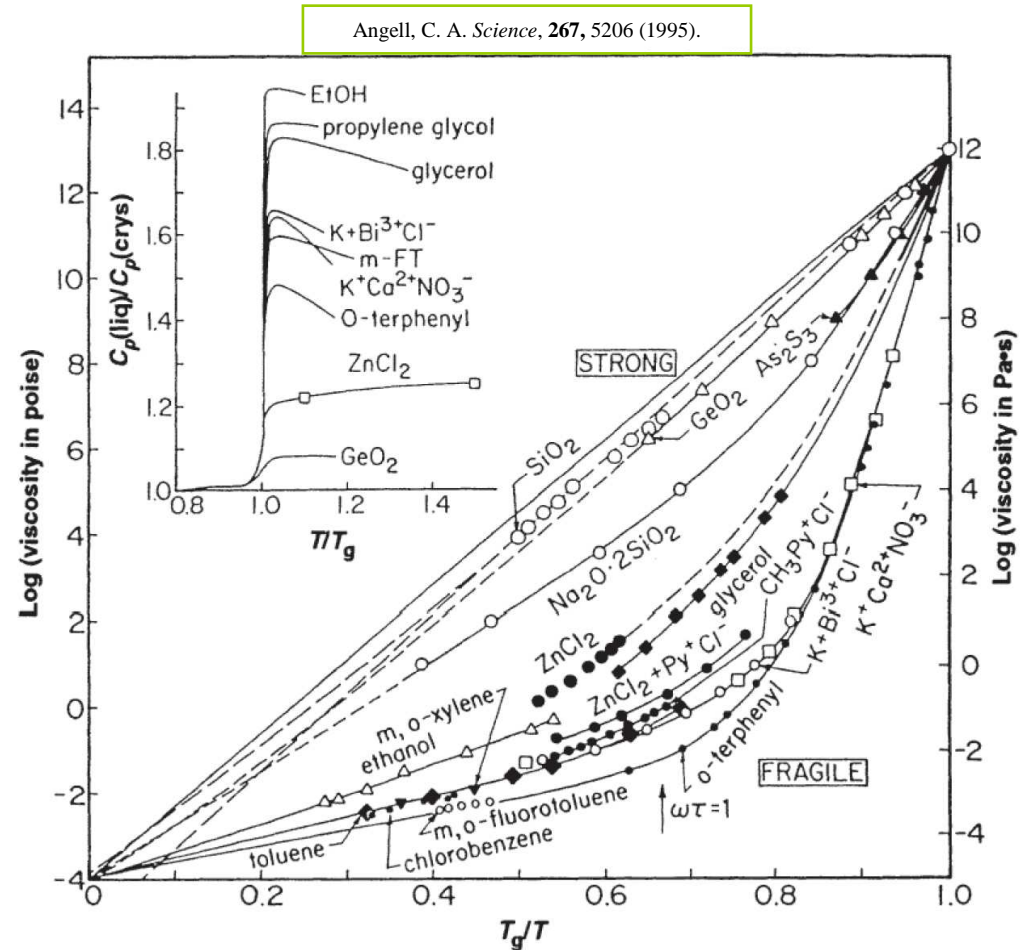
$$m = \left(\frac{d \ln(\eta)}{dT} \right)_{T=T_g}$$

$$\eta(T) = \eta_0 \exp\left(\frac{\Delta E_l}{k_B T} \right)$$

$$\frac{\Delta E_l}{T_g} = \frac{19.2^2 \ln 10}{m}$$

$$T_g \propto K_\infty + xG_\infty$$

A proposed linear correlation between the fragility and instantaneous Poisson ratio



Poisson Ratio Prediction

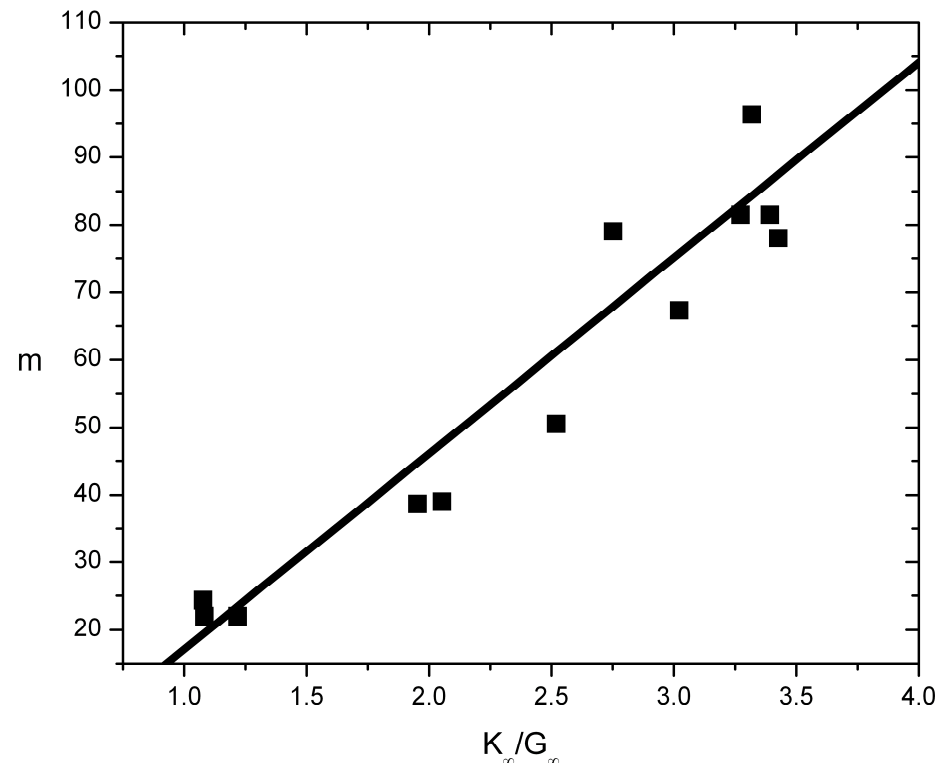
Novikov; Sokolov. *Nature* **431**, 961-963 (2004).

$$m = \left(\frac{d \ln(\eta)}{dT} \right)_{T=T_g}$$

$$\eta(T) = \eta_0 \exp\left(\frac{\Delta E_l}{k_B T} \right)$$

$$\frac{\Delta E_l}{T_g} = \frac{19.2^2 \ln 10}{m}$$

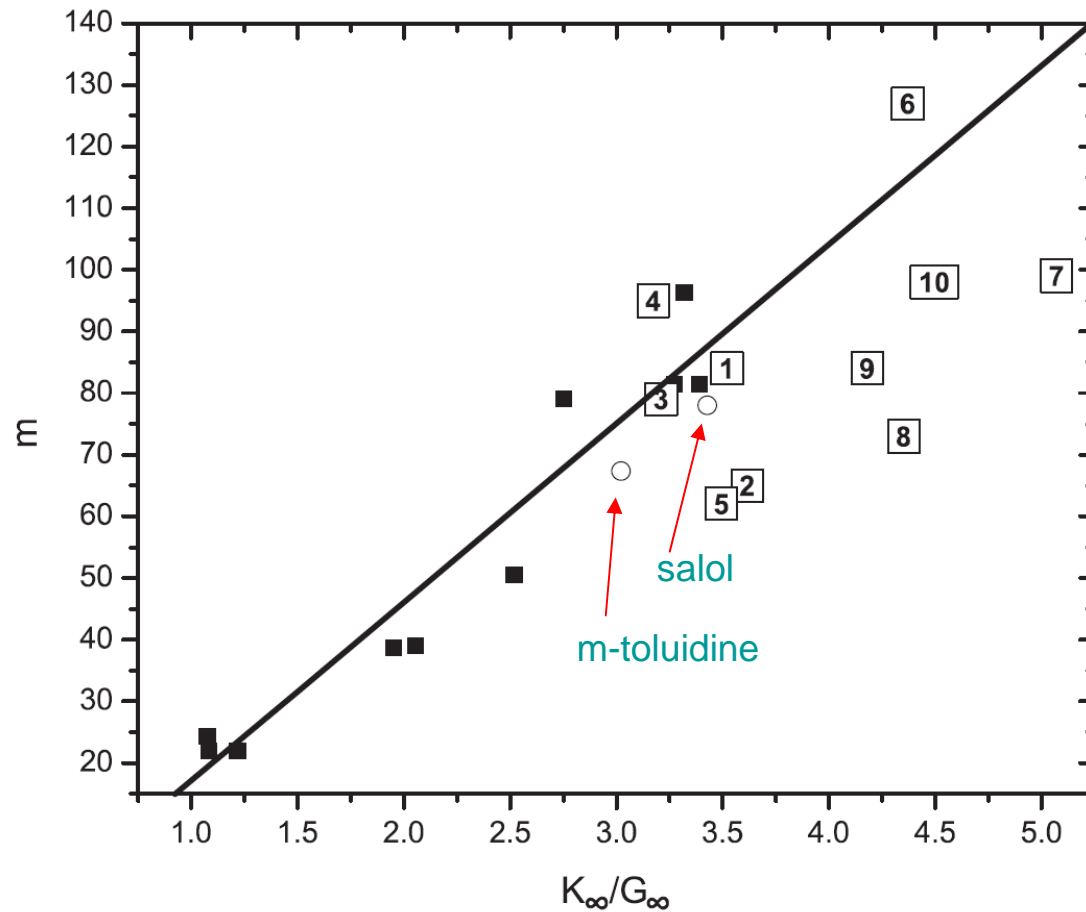
$$T_g \propto K_\infty + xG_\infty$$



A proposed linear correlation between the fragility and instantaneous Poisson ratio

$$m = 29 \left(\frac{K_\infty}{G_\infty} - 0.41 \right)$$

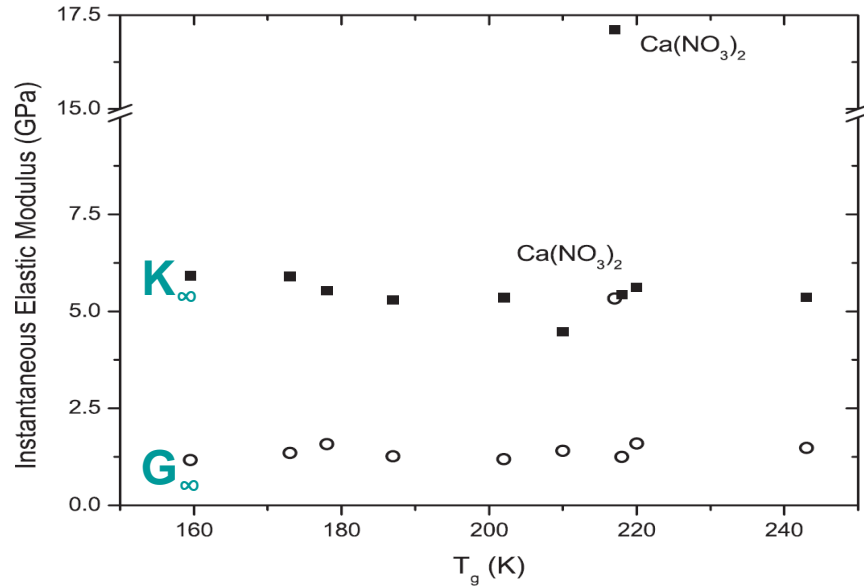
Poisson Ratio Prediction



1. 2BP₈₇/oTP₁₃
2. 5-phenyl 4-ether
3. Ca(NO₃)₂ 4H₂O
4. DC704
5. diethyl phthalate
6. m-fluoroaniline
7. propylene carbonate
8. salol
9. m-toluidine
10. triphenyl phosphite

Our results introduce more disagreement with the proposed correlation between fragility and the Poisson ratio.

Poisson Ratio Prediction



One proposed assertion is the linear relationship between the bulk and shear moduli and T_g .

$$T_g \propto K_\infty + xG_\infty$$

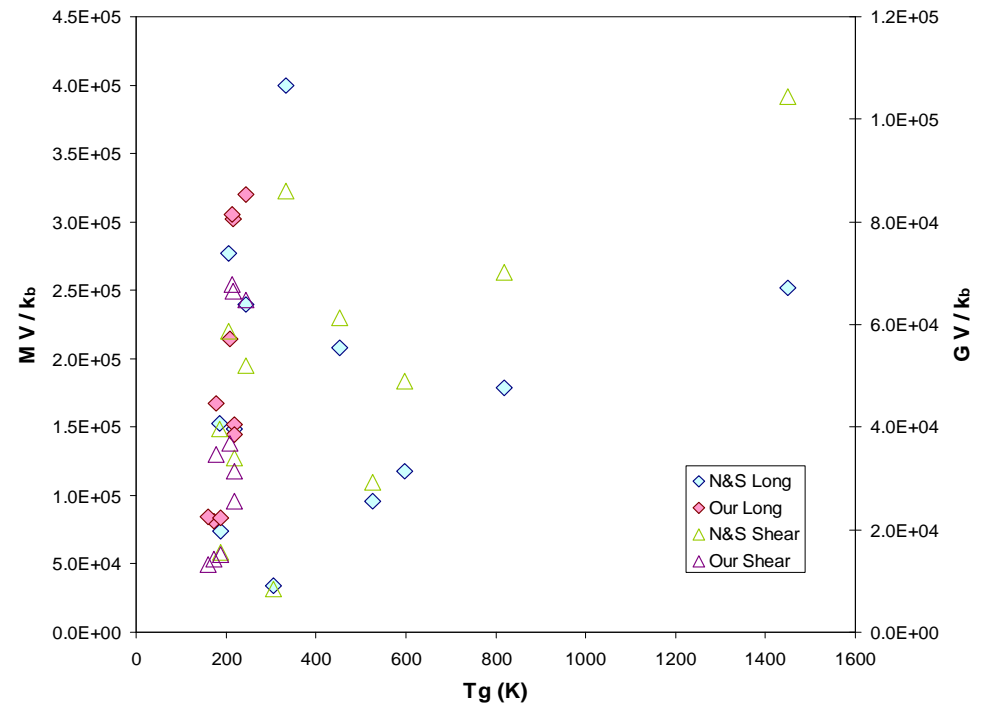
This assertion is not supported by our data

Egami *et al.* propose that the relationship should be

$$T_g \propto V \cdot (K_\infty + xG_\infty)$$

And they show this correlation for metallic glasses.

Egami *et al.* *Phys Rev B* **76**, 024203 (2007).



Outline

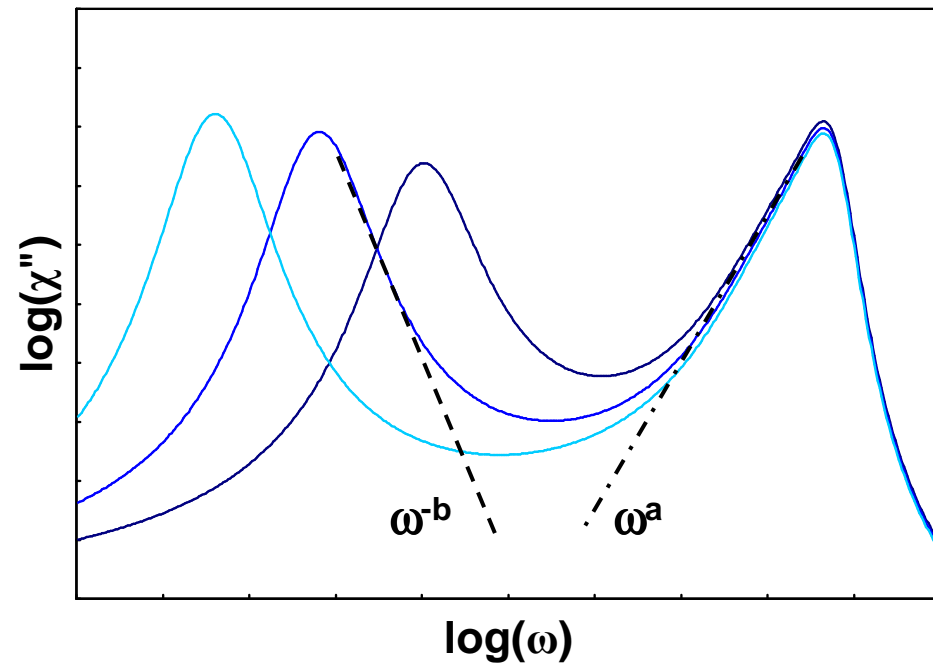
- Experimental
 - ISTS (longitudinal)
 - ISBS (shear and longitudinal)
 - Results and Tests of Theory
 - Shoving Model (shear)
 - Poisson Ratio (shear and longitudinal)
 - TPP (shear vs. longitudinal)
 - DC704 (longitudinal)
- } In preparation

Summary

- ISS allows generation and probing of coherent longitudinal and shear acoustic phonons in the MHz frequency regime
- This has allowed direct tests of the shoving model, the proposed correlation between Poisson ratio and fragility, and some aspects of MCT

Outlook

- Extend accessible acoustic frequency range of ISS to provide overlap between our two techniques and provide a large range of longitudinal (9-10 decades) and shear (4-5 decades) acoustic waves
- Allow test of MCT predicted relationship between 'a' and 'b' exponents



Comparison of MCT solution for $\chi''(\omega)$ with the two power laws. a is the exponent for the β -relaxation regime and b is the exponent for the α -relaxation regime.

Acknowledgements

- Prof. Keith Nelson
- Dr. Thomas Pezeril
- Christoph Klieber
- Dr. Darius Torchinsky
- Jeremy Johnson
- Kara Manke
- Stephan Andrieu, Univ. Poincaré

This work was supported in part by

- DOE Grant No DE-FG02-00ER15087
- NSF grants CHE-0616939
- DMR-0414895

Thank you for your attention!